

# GALEACYSTA ETRUSCA COMPLEX: DINOFLAGELLATE CYST MARKER OF PARATETHYAN INFLUXES TO THE MEDITERRANEAN SEA BEFORE AND AFTER THE PEAK OF THE MESSINIAN SALINITY CRISIS

SPERANTA-MARIA POPESCU  
UMR 6538, Domaines Océaniques  
Institut Universitaire Européen de la Mer  
Université de Bretagne Occidentale  
1, Place Nicolas Copernic  
29280 Plouzané, France  
e-mail: Speranta.Popescu@univ-brest.fr

FLORENT DALESME  
UFR des Sciences de la Terre  
Université Claude Bernard – Lyon 1  
Campus de La Doua  
Bâtiment Géode, 69622 Villeurbanne cedex, France  
e-mail: florent.dalesme@wanadoo.fr

GWÉNAËL JOUANNIC  
UMR 8148, Laboratoire Interactions et Dynamique  
des Environnements de Surface  
Université Paris-Sud  
Bâtiment 509  
91405 Orsay cedex, France  
e-mail: gwenael.jouannic@u.psud.fr

GILLES ESCARGUEL  
UMR 5125 PEPS, CNRS, France  
Université Claude Bernard – Lyon 1  
Campus de La Doua  
Bâtiment Géode, 69622 Villeurbanne cedex, France  
e-mail: Gilles.Escarguel@univ-lyon1.fr

MARTIN J. HEAD  
Department of Earth Sciences  
Brock University  
500 Glenridge Avenue  
St. Catharines  
Ontario L2S 3A1, Canada  
e-mail: mjhead@brocku.ca

MIHAELA CARMEN MELINTE-DOBRINESCU  
National Institute of Marine Geology and  
Geo-ecology (GEOECOMAR)  
23–25 Dimitrie Onciul Street  
024053 Bucharest, Romania  
e-mail: melinte@geoecomar.ro

MÁRIA SÜTO-SZENTAI  
Natural History Collection of Komlo  
Városház tér 1, 7300 Komlo, Hungary  
e-mail: suto.zoltanne@freemail.hu

KORALJKA BAKRAC  
Croatian Geological Survey  
HGI-CGS  
Sachsova 2  
10000 Zagreb, Croatia  
e-mail: Koraljka.Bakrac@hgi-cgs.hr

GEORGES CLAUZON  
C.E.R.E.G.E. (UMR 6635 CNRS)  
Université Paul Cézanne, Europôle de l'Arbois  
BP 80, 13545 Aix-en-Provence cedex 04, France  
e-mail: clauzon@cerege.fr

JEAN-PIERRE SUC  
UMR 5125 PEPS, CNRS  
Université Claude Bernard – Lyon 1  
Campus de La Doua  
Bâtiment Géode, 69622 Villeurbanne cedex, France  
e-mail: jean-pierre.suc@univ-lyon1.fr

## Abstract

More than one thousand specimens of a morphological complex including *Galeacysta etrusca* Corradini & Biffi 1988 from 11 Upper Miocene and Lower Pliocene localities of the Paratethyan and Mediterranean realms have been studied using a biometric approach in part relating to the degree of separation between endocyst and ectocyst. Four stable biometric groups have been distinguished statistically, the occurrence or prevalence of which appears closely linked to environmental conditions irrespective of the realm. Group 'a' is related to brackish conditions, group 'b' to marine conditions, group 'c' to freshwater, and group 'd' to high nutrient levels. Based on an accurate chronology provided by calcareous nannoplankton bioevents and recognition of the Messinian Erosional Surface, this study reveals:

- (1) the high sensitivity of the *Galeacysta etrusca* complex for reconstructing paleoenvironments and discriminating phases of connection and isolation of basins;
- (2) the detailed history of this species complex which originated in the Pannonian Basin at ca. 8 Ma before invading the Dacic Basin during the interval 6–5.60 Ma, then migrating into the Mediterranean during high sea-level connections (the ‘Lago Mare’ events just before and after the peak of the Messinian Salinity Crisis, i.e. at 5.60 Ma and during the interval ca. 5.46–5.278 Ma, respectively), and finally into the Black Sea at ca. 5.13 Ma;
- (3) an improved paleogeography for the Mediterranean and Paratethyan realms with focus on the location of corridors and the timing of when they were active.

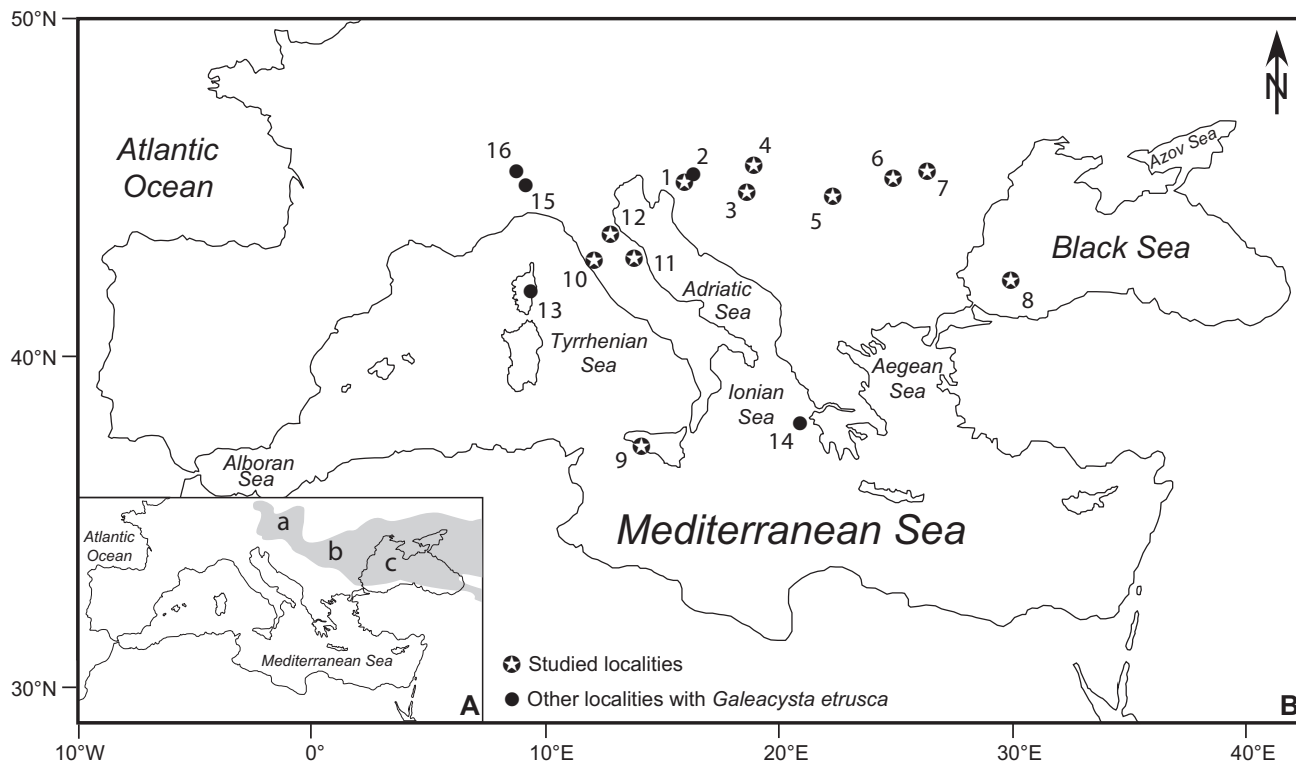
Based on field observations and dinoflagellate cyst data, we propose that the reflooding of the Mediterranean Basin by Atlantic waters occurred at ca. 5.46 Ma, about 130 kyr before the Zanclean GSSP (5.332 Ma).

**Key words:** *Galeacysta etrusca* complex; Paratethys–Mediterranean; Messinian; Zanclean; ‘Lago Mare’.

## INTRODUCTION

The dinoflagellate cyst *Galeacysta etrusca* Corradini & Biffi 1988 is considered to have migrated from the Paratethys into the Mediterranean Sea during the latest Messinian (Text-Figure 1A). It was first described from uppermost Messinian deposits at Cava Serredi (Livorno Province, Italy; Text-Figure 1B) by Corradini and Biffi (1988).

Morphologically similar dinoflagellate cysts are known from the Lower Pliocene of southern Romania as *Thalassiphora balcanica* Balteş 1971 and *Romanodinium areolatum* Balteş 1971; these differing from *Galeacysta etrusca* only by the reduced expression of their tabulation. Based on studies of the Pannonian Basin (Central Paratethys), Sütő-Szentai (1988) attempted to transfer *Thalassiphora balcanica* to the genus *Spiniferites*, although



Text-Figure 1. **A)** Paleogeographic location of the Paratethyan basins (in gray: a, Pannonian; b, Dacic; and c, Euxinian and Caspian) with respect to the present-day Mediterranean Sea. **B)** Localities yielding specimens of the *Galeacysta etrusca* complex: 1, Krašić; 2, Malunje; 3, Krajačići; 4, Majs 2; 5, Hinova; 6, Cernat; 7, Valea Vacii; 8, DSDP Site 380; 9, Eraclea Minoa; 10, Cava Serredi; 11, Maccarone; 12, San Donato; 13, Casabianda; 14, Aghios Sostis; 15, Torre Sterpi; 16, Sioneri.

the resulting combination was not validly published until later as *Spiniferites balcanicus* (Balteş 1971) Sütő-Szentai 2000. Sütő-Zoltáné (1994) maintained *Spiniferites balcanicus* and *Galeacysta etrusca* as separate species, but considered *Galeacysta etrusca* as a planktonic (thecate) form. *Nematosphaeropsis bicorporis* Sütőné-Szentai 1996 is also morphologically similar to *Galeacysta etrusca* and was described from the Upper Pannonian (regional Stage) in the Central Paratethys by Sütő-Szentai (1990). The name *Nematosphaeropsis bicorporis* was not validly published by Sütő-Szentai (1990) because the author did not state the location of the holotype. This information was later provided by the same author (under the name Sütőné Szentai, 1996), thereby completing requirements for valid publication.

Hence, *Galeacysta etrusca*, *Romanodinium areolatum*, *Spiniferites balcanicus*, and *Nematosphaeropsis bicorporis* are all validly published names relating to morphologically similar, if not identical, cyst forms. The spatial and temporal distributions of *Galeacysta etrusca*, *Romanodinium areolatum*, *Spiniferites balcanicus*, and *Nematosphaeropsis bicorporis* are associated with major paleogeographic changes that led to fragmentation of the Paratethys Sea (Text-Figure 1A) into separate basins (i.e. Pannonian, Dacic, Euxinian, and Caspian) as a result of the Carpathian uplift (Pomerol, 1973; Rögl and Steininger, 1983; Piller et al., 2007). This fragmentation implies important paleoenvironmental changes marked by a progressive decrease in salinity from west to east in these basins.

It has been demonstrated that dinoflagellates are sensitive to environmental change, and their cyst morphologies may become modified in response to environmental stress. The appearance of cruciform endocysts and variations in septal development (Wall et al., 1973; Wall and Dale, 1974) or reductions in process length (de Vernal et al., 1989; Dale, 1996; Ellegaard, 2000; Lewis et al., 1999; 2003; Head, 2007) have been correlated to the reduced salinities of surface waters. Laboratory experiments on living specimens have reproduced morphological changes observed in the fossil record, and show that certain species vary in process length (Kokinos and Anderson, 1995) and process morphology (Lewis and Hallett, 1997) even under stable salinity conditions, indicating that cyst morphological changes are controlled by multiple factors such as salinity, temperature, and nutrients.

The presence of morphologies transitional between *Galeacysta etrusca*, *Nematosphaeropsis bicorporis*, *Romanodinium areolatum*, and *Spiniferites balcanicus* suggests strongly that all these taxa are morphological variants of a single species. In this study, we therefore group them as the *Galeacysta etrusca* complex. We here-

after abbreviate the *Galeacysta etrusca* complex to *Galeacysta etrusca*, except when referring strictly to the morphotype described by Corradini and Biffi which we indicate as *Galeacysta etrusca* sensu stricto. We provisionally use the name *Galeacysta etrusca* Corradini and Biffi 1988 because the type material is illustrated and described unambiguously, although we acknowledge that the name *Romanodinium areolatum* Balteş 1971 has priority. The type materials of these morphotypes are under investigation, and formal synonymies will be presented in due course.

In the Pannonian Basin, the appearance of *Galeacysta etrusca* at about 8 Ma (Magyar et al., 1999a), followed by its high abundance up to ca. 5 Ma, allows this species complex to be considered as the marker for the uppermost regional biozone of the Upper Miocene (Sütő-Szentai, 1990; Magyar et al., 1999a; Müller et al., 1999; Sacchi and Horváth, 2002; Popov et al., 2006; Piller et al., 2007). In the Mediterranean area, *Galeacysta etrusca* occurred within the late Messinian–early Zanclean interval which includes the Messinian Salinity Crisis that led to the almost complete desiccation of the Mediterranean Sea. The regular occurrence of *Galeacysta etrusca* sensu stricto in these uppermost Messinian deposits explains why this species has become the microplankton reference for the ‘Lago Mare’ biofacies (Bertini et al., 1995).

The present study aims to show that during Messinian and Zanclean times, *Galeacysta etrusca* developed a wide range of morphological variability including (1) the degree of separation between ectocyst and endocyst representing the same morphological response to environmental stress as documented for process length in chorate dinoflagellate cysts, and (2) the overall size and length/width ratio of endocyst and ectocyst. This variability is documented in the present study using the biometric and statistical analysis of a data set based on 1144 specimens of *Galeacysta etrusca* from Central–Eastern Paratethys and Mediterranean sections located within the Upper Miocene and Lower Pliocene (Text-Figure 1B). We note that the shape of the endocyst, which varies from oval to cruciform, can also be important but this parameter was not documented in the present study. Two complementary aspects are particularly focused upon: (1) the geographic and hydrographic reconstruction of the Paratethys and Mediterranean realm around the Messinian Salinity Crisis, and (2) the morphological and biometric characterization of *Galeacysta etrusca* as a response to environmental changes. These two research themes lead us to address two main questions:

- (1) Is it possible to distinguish between the two ‘Lago Mare’ events evidenced by Clauzon et al. (2005) using

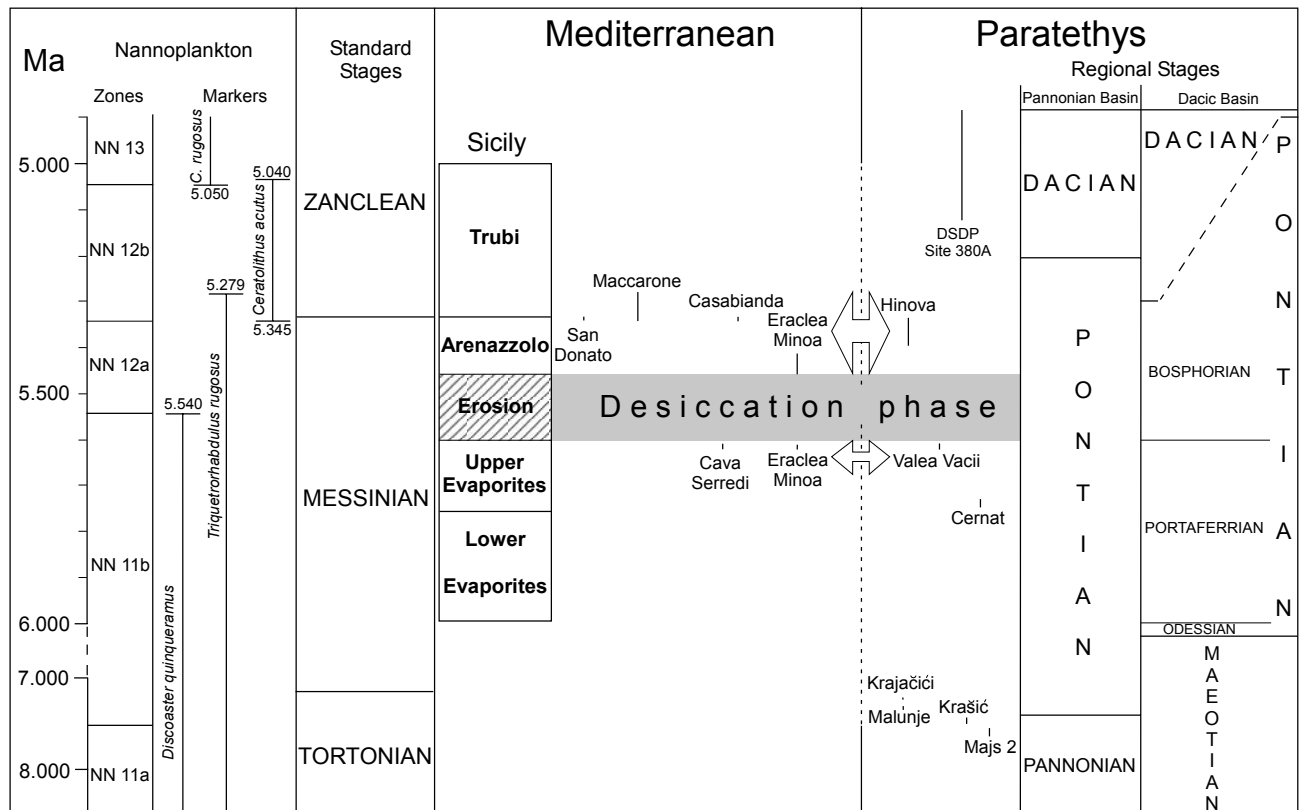
the biometric range of *Galeacysta etrusca* in the Mediterranean realm?

- (2) Do the inferred *Galeacysta etrusca* migrations give information about the complicated paleogeographical changes within the Mediterranean and Central–Eastern Paratethys regions during this period?

### THE MESSINIAN SALINITY CRISIS AND THE ‘LAGO MARE’ EVENTS

The Mediterranean experienced dramatic changes during the Late Miocene when it became temporarily isolated as a result of tectonic activity (Hsü et al., 1973; Duggen et al., 2003; Jolivet et al., 2006). Isolation led to the Messinian Salinity Crisis, peaking with a severe drop in Mediterranean sea-level which resulted in the deposition of thick evaporites in central basins (Hsü et al., 1973; Rouchy and Caruso, 2006) and intense subaerial erosion of the margins (Clauzon, 1999). During the almost complete desiccation of the Mediterranean Sea, the Paratethys was considered to be a suspended basin full of water (Hsü et al., 1978; Cita et al., 1978). The drainage of Paratethys into the Mediterranean Sea was considered as a single isochronous event by Hsü et al. (1973) as evidenced by the ‘Lago Mare’ biofacies characterized by Paratethyan fossil assemblages. This hypothesis was contradicted by (1) the discovery of latest Messinian and earliest Zanclean Mediterranean marine calcareous nannoplankton in the Eastern Paratethys (Dacic Basin: Mărunțeanu and Papaianopol, 1995; 1998; Drivaliari et al., 1999; Snel et al., 2006; Azov Sea: Semenenko and Olejnik, 1995) within the time-frame encompassing the Messinian Salinity Crisis; and (2) by the clear evidence of two successive falls in sea level (Clauzon et al., 1996), now generally accepted (CIESM, 2008). The first was from 5.960 to about 5.760 Ma, when a minor sea-level drop caused the deposition of evaporites in the more-or-less isolated marginal basins (gypsum, halite and potash salts in such areas as Sicily where they constitute the Lower Evaporites) and some erosion in the most proximal parts of river valleys. The second was from 5.60 to ca. 5.46 Ma when a major sea-level drop resulted in: (1) the almost complete desiccation of the Mediterranean Sea, (2) deposition of the central basin evaporites, and (3) massive subaerial erosion (deep river canyons and intense dismantling of the margins) that strongly cuts the marginal evaporites and extends to the central basin evaporites. These two sea-level drops were separated by an intermediate transgressive and cyclic episode corresponding to the Upper Evaporites of Sicily, where, as at Eraclea Minoa, relatively low sea-levels caused the deposition of six gypsum beds.

A severe erosion also impacted the Eastern Paratethys (Gillet et al., 2003; 2007; Clauzon et al., 2005), which had been connected almost continuously with the Mediterranean Sea during the high sea-level episodes of the Neogene since about 14 Ma (Mărunțeanu and Papaianopol, 1995; 1998). Popescu (2006) used the late arrival of marine dinoflagellate cysts at DSDP Leg 42, Site 380 in the Black Sea to demonstrate that the supposed ‘proto-Bosphorus’ was closed during the Late Neogene, and that the gateway was instead located in the Balkans area (Clauzon et al., 2005). The presence of Paratethyan organisms, namely (1) molluscs (dreissenids and lymnocyprids), (2) ostracods (*Cyprideis pannonica* group), and (3) dinoflagellate cysts (*Galeacysta etrusca*, *Spiniferites cruciformis*, *Pyxidinospsis psilata* etc.), in the Mediterranean (Clauzon et al., 2005); simultaneously with the presence of Mediterranean planktonic microorganisms, namely (1) calcareous nannoplankton (Mărunțeanu and Papaianopol, 1995, 1998; Semenenko and Olejnik, 1995; Clauzon et al., 2005; Snel et al., 2006), (2) foraminifers, and (3) dinoflagellate cysts (Popescu, 2006; Popescu et al., 2006), in the Paratethys implies that these two seas communicated during high sea levels before and after the Messinian Salinity Crisis. This connection resulted in two ‘Lago Mare’ events, the first indicated at the top of the Messinian marginal evaporites and the second in the lowermost Zanclean (Clauzon et al., 2005). These observations have led to the new concept of the ‘Lago Mare’ events (Clauzon et al., 2005) depicted in Text-Figure 2. When contrasting the various concepts related to the term Lago Mare, we use inverted commas when referring to the distinctive Mediterranean biofacies or its corresponding event relating to the invasion of Paratethyan organisms into the Mediterranean (two high sea-level exchanges, and an intermediate dilution episode; see Clauzon et al., 2005 for details), and we use the term without inverted commas when referring to a stratigraphic formation described as such. These two ‘Lago Mare’ events accord with the two-step scenario of Clauzon et al. (1996, 2005), as summarized above. This scenario contrasts with: (1) Krijgsman et al.’s (1999) scenario which considers the marginal evaporites as coeval with the central basin evaporites without any sea-level fall at the beginning of the crisis (in addition to a discrepancy over the precise location of the erosional surface in Sicily), (2) Rouchy and Caruso’s (2006) scenario that invokes multiple erosional phases even though a single erosional event is marked at the Mediterranean margins (Lofi et al., 2005), and (3) Braga et al.’s (2006) scenario where the marginal pre-evaporitic paleotopography is confused with the Messinian Erosional Surface which everywhere postdates the marginal evaporites (Clauzon et al., 1996).



Text-Figure 2. Chronostratigraphic position of localities yielding specimens of the *Galeacysta etrusca* complex, based on the two-step scenario of the Messinian Salinity Crisis (Clauzon et al., 1996; 2005). Calcareous nannoplankton biochronology is from Lourens et al. (2005) amended by Raffi et al. (2006). Age boundaries of regional stages in the Dacic Basin reflect discrepancies between authors (Vasiliev et al., 2004; Clauzon et al., 2005; Popescu et al., 2006; Snel et al., 2006; Stoica et al., 2007). Age boundaries of regional substages in the Dacic Basin are after Snel et al. (2006). Double arrows specify major episodes of interconnection ('Lago Mare' events; Clauzon et al., 2005) between the Mediterranean and Paratethys within a phase of discontinuous water exchanges as indicated by the dashed line separating the Mediterranean and Paratethys columns.

## LOCALITIES STUDIED AND THEIR CHRONOSTRATIGRAPHIC SETTING

According to Clauzon et al. (2005), two episodes of water exchange existed between the Mediterranean and Paratethys seas during 6–5 Ma, each high sea-level connection generating a 'Lago Mare' biofacies on the Mediterranean margins (Bertini et al., 1995). The first episode preceded the desiccation phase of the Messinian Salinity Crisis and coincides with the NN11b calcareous nannoplankton subzone (Text-Figure 2). At its highest intensity this exchange caused the arrival of *Galeacysta etrusca* sensu stricto as recorded at Cava Serredi, Eraclea Minoa (the first influx), and Aghios Sostis. The second episode immediately followed the desiccation phase of the Messinian Salinity Crisis during the late NN12a and earliest NN12b calcareous nannoplankton subzones (Text-

Figure 2). The resulting invasion of *Galeacysta etrusca* lasted about 130 kyr (as calculated at Eraclea Minoa between ca. 5.46 Ma for the base of the Arenazzolo Formation and that of the base of the acme of *Sphaeroidinellopsis*; Lourens et al., 2005), while the two-way water-exchange continued sporadically until ca. 5 Ma as evidenced at DSDP Site 380 (Popescu, 2006) (Text-Figure 2).

In this study, we examined 14 localities (Majs 2, Krajačići, Krašić, Cernat, Valea Vacii, Eraclea Minoa, Hinova, Maccarone, San Donato, DSDP Site 380, Malunje, Torre Sterpi, Sioneri, and Casabianda) distributed along the Central and Eastern Paratethys and Mediterranean margins. The last four localities were not retained for final statistical analyses and comparisons because *Galeacysta etrusca* is scarce. The chronostratigraphic positions of the localities studied are reported below.

### The Central Paratethys (Pannonian Basin)

The earliest appearance of *Galeacysta etrusca* is at 8 Ma in the Pannonian Basin (Central Paratethys) where it persisted for 3 Myr, until ca. 5 Ma. This species has been used as a chronostratigraphic indicator throughout the Pannonian Basin (Magyar et al., 1999a, b; Müller et al., 1999). Because the Late Miocene stratigraphy of this basin is debated (Sacchi and Horváth, 2002; Piller et al., 2007), we follow the traditional approach that does not recognise the Pontian Stage in the Pannonian Basin (Magyar et al., 1999a; Müller et al., 1999) (Text-Figure 2).

In this basin, four localities were selected in order to observe (1) the morphology of the 'oldest' representatives of *Galeacysta etrusca* in typical low-salinity paleoenvironments (Majs 2 section), and (2) possible morphological modifications related to increasing salinity as indicated by the presence of marine dinoflagellate cysts (Malunje, Krašić and Krajačić sections) and nannoplankton (Krajačić). The **Majs 2** samples analyzed in this study have been selected from the oldest beds of the *Galeacysta etrusca* Zone at ca. 8 Ma (Text-Figure 2; Magyar et al., 1999a, b). The low-salinity paleoenvironments at this time are indicated by the presence of typically Paratethyan dinoflagellate cyst assemblages and the absence of marine dinoflagellates cysts. The **Malunje**, **Krašić** and **Krajačić** sections of the Pannonian Basin belong to the *Spiniferites validus* biozone (Magyar et al., 1999a; Kováčic et al., 2004). The presence of marine microorganisms suggests a connection between the Pannonian Basin and Mediterranean Sea at that time.

### The Eastern Paratethys (Dacic and Euxinian basins)

In the Eastern Paratethys (Dacic and Euxinian basins), *Galeacysta etrusca* is a common species in sediments of the regional Pontian Stage (Text-Figure 2). In spite of intensive efforts using magnetostratigraphy in conjunction with molluscan biostratigraphy, the ages of regional stage boundaries in the Dacic Basin are still disputed (Maeotian–Pontian: 6.15–5.75 Ma; Pontian–Dacian: 5.30–4.90 Ma; Vasiliev et al., 2004; Snel et al., 2006; Stoica et al., 2007; see also Clauzon et al., 2005; Popescu et al., 2006); discrepancies are indicated on Text-Figure 2. Ages of the regional substage boundaries have been proposed only by Snel et al. (2006) and are reported for indicative purposes in Text-Figure 2: 6.0 Ma for the Odessian–Portaferrian and 5.60 Ma for the Portaferrian–Bosphorlian. In this study, we chronologically calibrate the sections using global nannoplankton biostratigraphy and consider their position with respect to the Messinian Erosional Surface identified in both basins. Four localities were analyzed in these two basins, respectively Cernat, Valea Vacii and Hinova in the

Dacic Basin, and DSDP Site 380 in the Black Sea (Euxinian Basin). The **Cernat** and **Valea Vacii** sections (Text-Figure 2) belong to the Portaferrian and Bosphorlian substages, respectively. Both sections contain calcareous nannoplankton of the NN11b subzone (Măruntănu and Papaianopol, 1998; Snel et al., 2006), since the basin at that time was connected to the Mediterranean (Clauzon et al., 2005), and are considered Late Messinian in age. The **Hinova** section contains a Bosphorlian mollusc fauna and includes calcareous nannoplankton assignable to subzone NN12a (Popescu, 2001; Clauzon et al., 2005; Popescu et al., 2006). More precisely, they are astronomically dated at 5.40 to 5.34 Ma based on vegetation cycles identified in the pollen record (Popescu et al., 2006) (Text-Figure 2). This section overlies a massive erosional surface referred to the desiccation phase of the Messinian Salinity Crisis (Clauzon et al., 2005). Sediments from the Black Sea **DSDP Site 380** considered in this study overlie the Messinian Erosional Surface (Gillet et al., 2007) and cover an astronomically dated time-window between 5.11 and 5.00 Ma, as also indicated by the pollen record (Popescu, 2006) (Text-Figure 2).

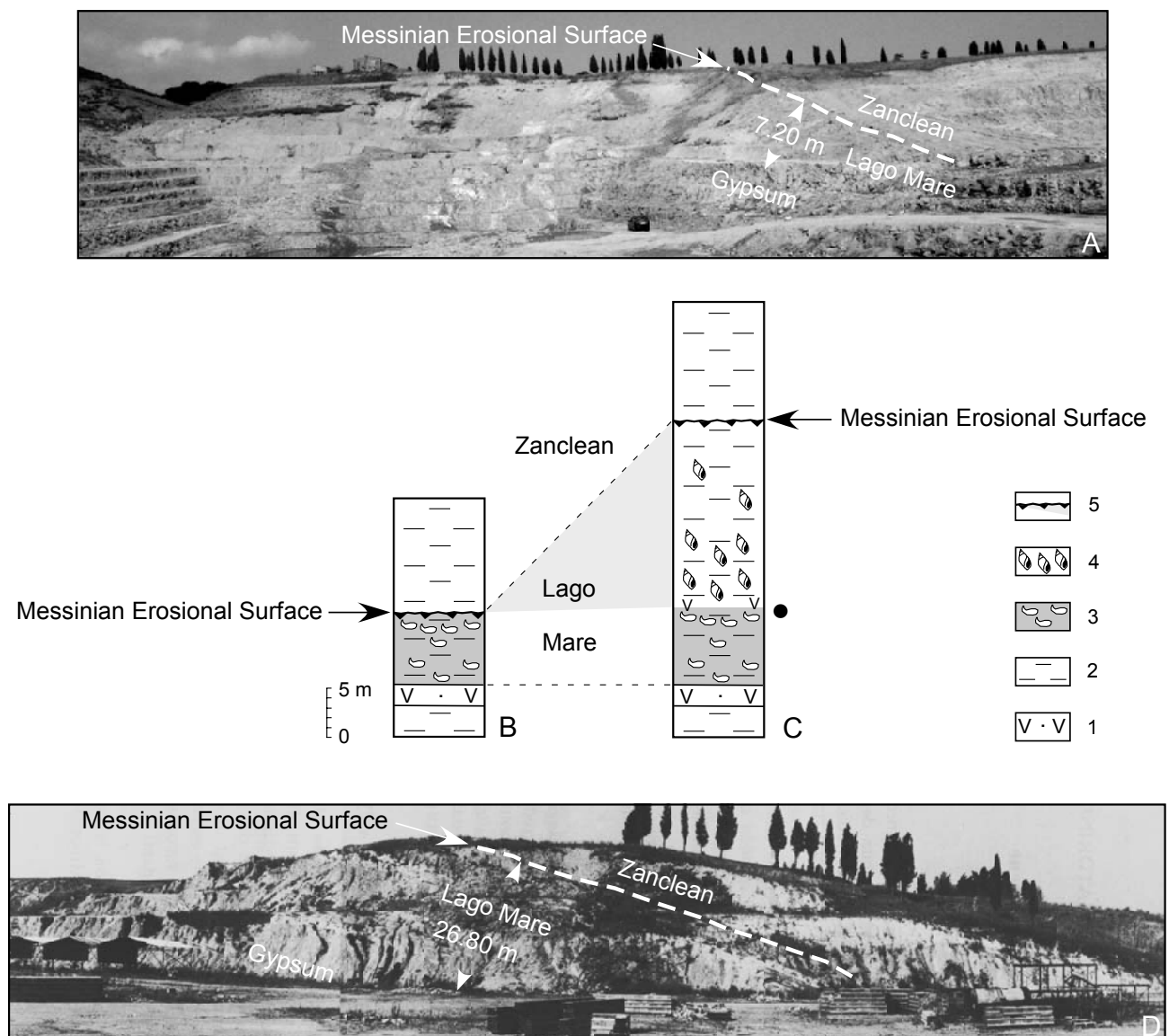
### The Mediterranean Realm

Along the Mediterranean margins, *Galeacysta etrusca* is recorded in Central Italy at Cava Serredi (Corradini and Biffi, 1988), Maccarone (Bertini, 2006; Popescu et al., 2007), and San Donato (Bassetti, 1997); in Northern Italy at Torre Sterpi and Sioneri (S.-M. Popescu, unpublished); in Sicily at Eraclea Minoa (Londeix et al., 2007); and in Corsica at Casabianda (S.-M. Popescu, unpublished) (Text-Figure 1B). Based on their biostratigraphy and position relative to the Messinian Erosional Surface (Text-Figure 1B), Cava Serredi and Aghios Sostis are considered Messinian localities, corresponding to the first 'Lago Mare' event (Clauzon et al., 2005). In contrast, Maccarone, San Donato, Torre Sterpi, Sioneri and Casabianda are post Messinian Salinity Crisis localities and correspond to the second 'Lago Mare' event (Clauzon et al., 2005). A special case is the Eraclea Minoa section that includes both 'Lago Mare' events. The Cava Serredi, Eraclea Minoa, Maccarone, and Casabianda sections were restudied in order to refine their chronostratigraphic positions with respect to the Messinian Salinity Crisis. The newly obtained bio- and chronostratigraphic data are presented below.

At the **Cava Serredi** quarry, a Lago Mare deposit about 26 m thick was described in the 1980s, sandwiched between a thick uppermost gypsum bed and Zanclean clays (Bossio et al., 1981). It was clearly subdivided into two parts: a lower 7.50-m thick dreissenid-rich part, which includes some highly concentrated beds (coquinas), is

considered to indicate brackish conditions; and an upper part, about 18 m thick and rich in *Melanopsis* and *Theodoxus* shells, corresponds to a more freshwater environment (Text-Figure 3A, B; Bossio et al., 1981). Today, the working face of the quarry has moved about 2 km northward, and only 6.60 m of Lago Mare separates the highest gypsum bed from the lowermost Zanclean clays. These clays are well characterized by our lowest record of *Ceratolithus acutus*

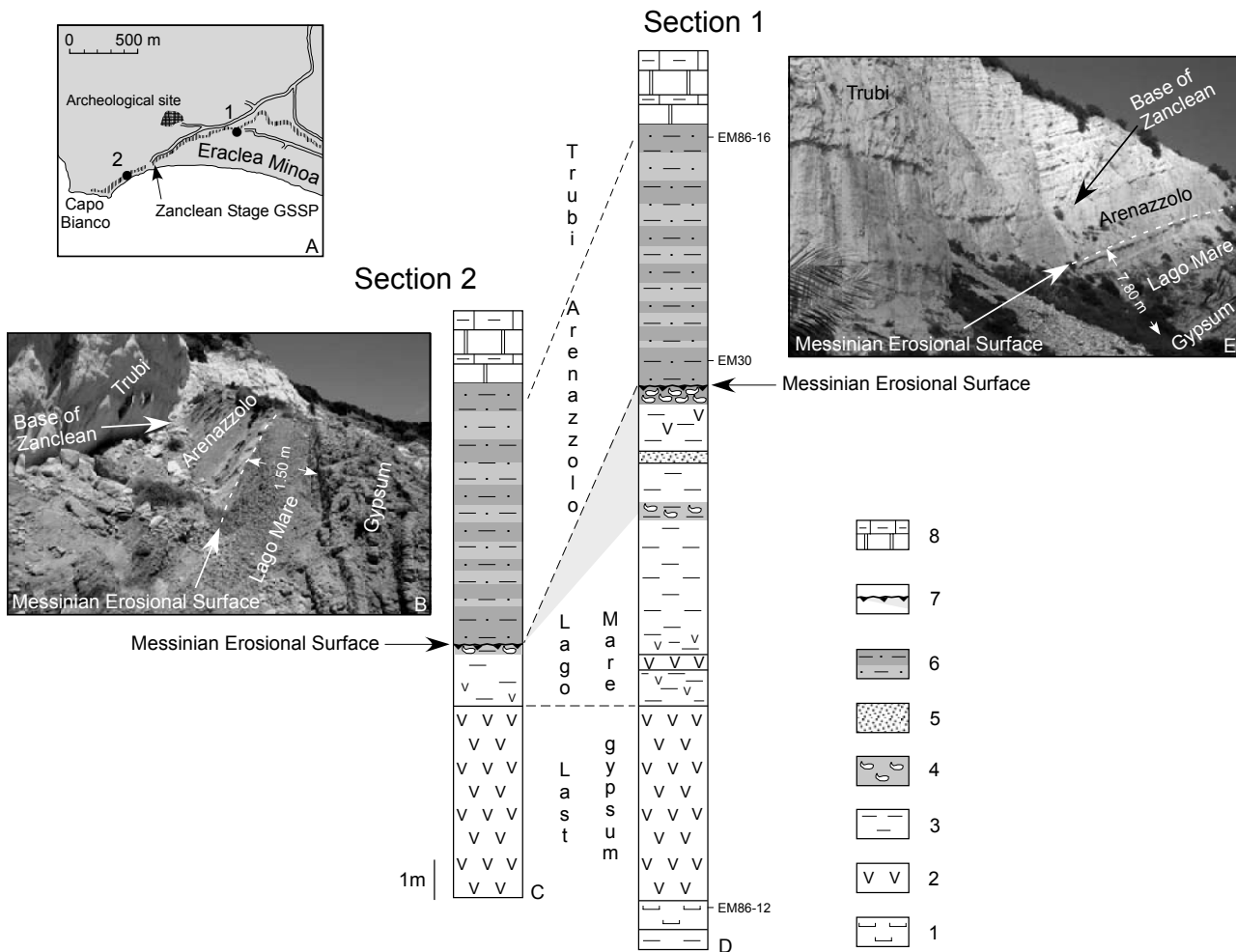
occurring 3 m above their base, this datum preceding that of *Sphaeroidinellopsis* as reported by Bossio et al. (1981) (Text-Figure 3B, C). The Lago Mare comprises only dreissenid-rich sediments, including coquinas. The *Melanopsis* layer is absent. We conclude that the missing ca. 19 m of Lago Mare (i.e. the entire *Melanopsis* layer plus ca. 1 m of dreissenid-rich sediment) were eroded during the desiccation phase of the Messinian Salinity Crisis and that,



Text-Figure 3. Stratigraphy of the upper Messinian and lowermost Zanclean deposits at Cava Serredi in the early 1980s compared to the year 2005, with the location of the Messinian Erosional Surface. **A)** Photograph of the 2005 working face of the quarry (photo: J.-P. Suc). **B)** Section in 2005. **C)** Section published by Bossio et al. (1981) with the black circle indicating the *Galeacysta etrusca* sensu stricto layer. **D)** Photograph showing the working face of the quarry in the early 1980s (photo: A. Bossio). Key: 1, gypsum; 2, clay; 3, dreissenid bed; 4, *Melanopsis* bed; 5, Messinian Erosional Surface. Light gray shading indicates eroded sediments missing from the present-day working face of the quarry.

accordingly, the Messinian Erosional Surface corresponds here to moderate erosion and must be placed at the top of the Lago Mare (Text-Figure 3). This section was presented as showing a continuous passage from the Messinian to Zanclean by Bossio et al. (1981), Corradini and Biffi (1988), and Carnevale et al. (2006). In fact, the *Galeacysta etrusca* sensu stricto layer of the Cava Serredi locality documents what we consider an episode of high sea-level and intensive exchange between the Mediterranean and Eastern Paratethys just before the Mediterranean desiccation phase (Text-Figure 2) (Clauzon et al., 2005). The marine conditions of the Cava Serredi dreissenid beds have been supported recently by the presence of marine fish remains (Carnevale et al., 2006).

**Eraclea Minoa** is the only Mediterranean section where *Galeacysta etrusca* has been recorded before and after the Messinian desiccation phase (Clauzon et al., 2005; Londeix et al., 2007). Here, the desiccation is not expressed by well-marked erosion, probably because the locality occupied an interfluvial position in a semi-arid area (Suc and Bessais, 1990; Fauquette et al., 2006). However, a discontinuity has been reported as shown in Text-Figure 4. Two sections have been examined near the global stratotype section and point (GSSP) of the Zanclean Stage (Van Couvering et al., 2000) (Text-Figure 4A). Section 1 starts with clays and diatomitic turbidite underlying the highest gypsum bed of the Sicilian Upper Evaporites, followed by the clayey Lago Mare Formation (7.80 m thick) including



Text-Figure 4. Eraclea Minoa sections 1 and 2. **A**) Location of sections studied and of the Zanclean Stage global stratotype section and point (GSSP) (Van Couvering et al., 2000). **B**) Photograph of section 2 (photo: J.-P. Suc). **C**) Stratigraphic succession of section 2. **D**) Stratigraphic succession of section 1 showing the position of three samples from which specimens of the *Galeacysta etrusca* complex have been studied. **E**) Photograph of section 1 (photo: J.-P. Suc). Key: 1, diatomitic turbidite; 2, gypsum; 3, clays; 4, dreissenid coquina; 5, sand; 6, light–dark cycles within silts of the Arenazzolo Formation; 7, Messinian Erosional Surface; 8, carbonate–marly cycles of the Trubi Formation. Light gray shading indicates eroded sediments missing from section 2.

in its upper part three characteristic layers (two main dreissenid coquinas, 25 cm and 40 cm thick respectively, and between them a white sand 32 cm thick; Gautier, 1994). This is followed by the silty Arenazzolo Formation (5.60 m thick) comprising 6.5 dark–light cycles, itself overlain by the cyclic carbonate–marly Trubi Formation. The base of the Zanclean is placed at the base of the Trubi Formation (Text-Figure 4B, E). Nannoplankton assemblages from the Lago Mare Formation contain, inter alia, *Amaurolithus amplificus*, *Amaurolithus primus*, *Coccolithus pelagicus*, *Helicosphaera carteri* s.l., *Helicosphaera intermedia*, *Pontosphaera multipora*, small-sized reticulofenestrads, *Reticulofenestra pseudoumbilicus*, *Sphenolithus abies/moriformis* group, *Triquetrorhabdulus striatus* and *Triquetrorhabdulus rugosus*, and may be assignable to subzone NN11b. *Galeacysta etrusca* has been reported only from the diatomitic turbidite underlying the highest gypsum and within the Arenazzolo Formation (Londeix et al., 2007). We studied specimens from three samples, one from the diatomitic turbidite and two from the Arenazzolo Formation (Text-Figure 4D). Section 2 shows major lithological differences when compared with section 1: (1) the Lago Mare Formation is significantly reduced (1.50 m thick only) and shows only part of the lower dreissenid coquina at its top (Text-Figure 4C), and (2) the Arenazzolo deposits clearly onlap the Lago Mare clays (Text-Figure 4B). We suggest that the upper part of the Lago Mare of section 1 has been eroded in section 2. As a consequence, we place the Messinian Erosional Surface at the top of the Lago Mare Formation, an assumption also supported by the onlapping nature of the Arenazzolo silts (indicated in Corn e et al., 2004). Section 1, which has been inaccessible since 2001 because of the building of a wall, was described in detail by one of us (J.-P.S) and published in Gautier (1994: p. 64) and Londeix et al. (2007). This description when compared with the residual sediments of section 2 (Text-Figure 4C, D) allows us to demonstrate that erosion caused the observed difference. This proposal is fully consistent with new offshore data from the Strait of Sicily which sharply contradict the proposed Messinian erosion in Sicily (El Euch–El Koundi et al., 2009) as sandwiched between the Lower and Upper Evaporites (Butler et al., 1995; Krijgsman et al., 1999), an interpretation resulting from confusion with the effects of local tectonics (Clauzon et al., 1996; El Euch–El Koundi et al., 2009). In agreement with Decima and Wezel (1971) and Brolsma (1975; 1976), we consider that the Arenazzolo Formation represents the reflooding of the Mediterranean Basin by Atlantic waters, recorded below the base of the Trubi Formation, i.e. earlier than the Zanclean GSSP. The related time-interval should be about 130 kyr, taking the

6.5 dark–light cycles of the Arenazzolo Formation as precessional cycles just as those of the immediately overlying Trubi Formation (Hilgen and Langereis, 1993). Hence, the base of the Arenazzolo Formation would date from ca. 5.46 Ma, representing the age of Mediterranean reflooding after the Messinian Salinity Crisis (Text-Figure 2), an assumption consistent with the new concept of the ‘Lago Mare’ events as representing repeated exchanges during high sea-level between the Mediterranean and Paratethys (Clauzon et al., 2005). The *Galeacysta etrusca* occurrences at Eraclea Minoa are limited to episodes of rising sea-level represented by the diatomitic turbidite and Arenazzolo Formation (Londeix et al., 2007). We consider these episodes to have immediately preceded and followed the peak of the Messinian Salinity Crisis.

At **Maccarone** (Adriatic realm), *Galeacysta etrusca* has been recorded within a stratigraphic interval including the uppermost Di Tetto, Colombacci, and lowermost Argille Azzurre formations (Bertini, 2006; Popescu et al., 2007). The studied specimens are from the uppermost Di Tetto (samples 15–18) and Colombacci (samples 30–42) formations (Popescu et al., 2007; Table 1). The Argille Azzurre Formation characterizes the beginning of the Zanclean in the area (Selli, 1973) but the recent recording of *Ceratolithus acutus* both in the uppermost Di Tetto and entire Colombacci formations significantly lowers the reflooding by marine waters in this stratigraphic succession (Popescu et al., 2007). As a consequence, all the specimens of *Galeacysta etrusca* from the Maccarone section are younger than the Messinian Salinity Crisis (Text-Figure 2).

The studied *Galeacysta etrusca* specimens from **San Donato** belong to the upper Colombacci Formation (Bassetti, 1997) and accordingly refer to the same episode (Text-Figure 2). A similar stratigraphic position characterizes the **Torre Sterpi** locality near Tortona (Corselli and Grecchi, 1984) and the **Sioneri** locality near Alba (Cavallo and Repetto, 1988).

At **Casabianda**, the Aleria Formation overlies an erosional surface (Saint Martin et al., 2007) that we refer to the Messinian Erosional Surface because of our discovery of *Ceratolithus acutus* (accompanied, inter alia, by *Triquetrorhabdulus rugosus*) within the diatomitic sediments directly overlying those containing dreissenids and *Galeacysta etrusca*. The Casabianda diatomites were obviously deposited after the end of the Messinian Salinity Crisis (Text-Figure 2).

## METHODS

Within the above chronostratigraphic framework, 47 samples (Table 1) were selected from most of the localities

TABLE 1. Samples studied and their respective sections and nannoplankton biostratigraphic assignment.

Region	Locality	Samples	Nannoplankton	References	
<b>Eastern Paratethys</b>	Dacic Basin	Hinova	H0, H1a, b, c, d, e H2, H2a, b, c, d, e H2f, g	Subzone NN12a	Popescu et al. (2006) Clauzon et al. (2005)
	Euxinian Basin	DSDP Hole 380A (depth in m)	828.02, 829.06, 837.06, 839.08, 840.07, 841.91	No	Popescu (2001; 2006)
<b>Mediterranean</b>	Casabianda	CO.08 (Aleria Formation)		Subzone NN12b	Saint Martin et al. (2007)
	San Donato	SD21 (Colombacci Formation)		Not searched	Bassetti (1997)
	Maccarone	38, 41, 42 (Colombacci Formation) 34, 35, 36 (Colombacci Formation) 30, 31, 33 (Colombacci Formation) 15, 16, 17, 18 (Di Tetto Formation)		Subzones NN12a and b	Popescu et al. (2007)
	Eraclea Minoa	EM86-16, EM30 (Arenazzolo Formation) EM86-12 (diatomitic turbidites underlying the highest gypsum)		Subzone NN12a Subzone NN11b	
	Cava Serredi	7.2 of Corradini and Biffi (1988)		Subzone NN11b	Bossio et al. (1981)
<b>Eastern Paratethys</b>	Dacic Basin	Cernat	P1, P4	Subzone NN11b	Mărunțeanu and Papaianopol (1998)
		Valea Vacii	3, 4	Subzone NN11b	Snel et al. (2006)
<b>Central Paratethys</b>	Pannonian Basin	Krajačići	Krajačići I 1/1, 1/3	Undiagnostic	Kováčic et al. (2004)
		Krašić	Krašić I 1/1	No	Kováčic et al. (2004)
		Malunje	MAL I 1/1	No	Magyar et al. (1999a)
		Majs 2 (depth in m)	257.3	No	Sütő Zoltánné (1994)

discussed (Majs 2, Krajačići, Krašić, Cernat, Valea Vacii, Eraclea Minoa, Hinova, Maccarone, San Donato and DSDP Site 380). Measurements from Malunje, Torre Sterpi, Sioneri and Casabianda were not retained for final statistical analyses and comparisons because *Galeacysta etrusca* is scarce at these localities. We did not examine the *Galeacysta etrusca* specimens from Aghios Sostis. We did not recover the *Galeacysta etrusca* sensu stricto horizon at Cava Serredi at the top of the dreissenid layers in the present-day working face of the quarry, as it was probably eroded during the desiccation phase (Text-Figure 3). Hence, we used for this locality the photographs published by Corradini and Biffi (1988).

Each sample (20 g of dry sediment) was processed using standard methods (Cour, 1974): acid digestion, concentration using  $ZnCl_2$  (at density 2.0), and sieving at 10  $\mu m$ . A 50- $\mu l$  volume of residue was mounted between coverslip

and microscope slide using glycerine in order to allow rotation of dinoflagellate cysts for their complete examination and the acquisition of consistent measurements. Specimens were measured using a light microscope at 600 $\times$  and 1000 $\times$  magnifications.

For each specimen we took four measurements (Plate 1): the length and width of the endocyst ( $L_{EN}$  and  $W_{EN}$ , respectively) and the length and width of the ectocyst ( $L_{EC}$  and  $W_{EC}$ , respectively). To obtain consistent measurements, all specimens were rotated into dorso-ventral orientation. Based on these four log-transformed variables, we first performed a one-way Multiple Analysis of Variance between all the sections studied (complete data set: 1,144 individuals) coupled with a Canonical Variate Analysis (a multigroup Discriminant Analysis; Text-Figure 5) (Legendre and Legendre, 1998). Log-transformation was used in order to normalize initially right-skewed distribu-

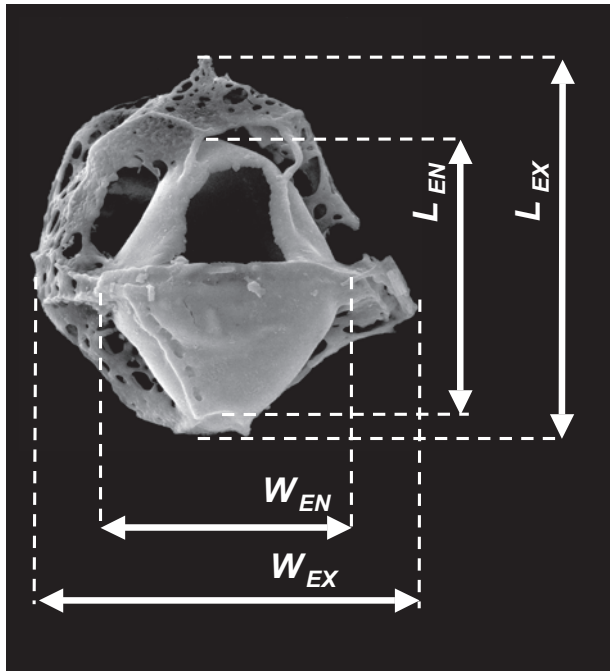


PLATE 1

The four measured parameters shown on a specimen of the *Galeacysta etrusca* complex.  $L_{EN}$ , length of endocyst;  $W_{EN}$ , width of endocyst;  $L_{EC}$ , length of ectocyst;  $W_{EC}$ , width of ectocyst. The scale bar represents 20  $\mu\text{m}$ .

tions and to linearize possible allometric relations within the biometric space. This preliminary analysis returned highly significant results indicating two main sources of biometric variation between samples: the overall dinocyst size on the first canonical variate axis, and the relative size of ectocyst vs. endocyst on the second canonical variate axis.

We thus defined two simple log-transformed synthetic descriptors:

$$X = \log\left(\sqrt[4]{L_{EN} \times W_{EN} \times L_{EC} \times W_{EC}}\right), \quad \text{and}$$

$$Y = \log(D_{EN/EC}) = \log\left(\frac{L_{EN} \times W_{EN}}{L_{EC} \times W_{EC}}\right) = \log(L_{EN} \times W_{EN}) - \log(L_{EC} \times W_{EC})$$

$X$  is the log-transformed geometric mean of the four initial variables; it is an estimate of the overall size of the dinoflagellate cyst.  $Y$  is the log-transformed ratio (i.e. the Simpson Ratio; see Simpson et al., 1960, p. 356–358) of the endocyst and ectocyst length and width products (i.e. the  $D_{EN/EC}$  ratio, expressed as a percentage of the ectocyst's length  $\times$  width), allowing the comparison of the relative (not absolute) dimensions of these two cyst structures.  $Y$  directly co-varies with the relative distance between ectocyst and endocyst: all sizes being equal, the greater the

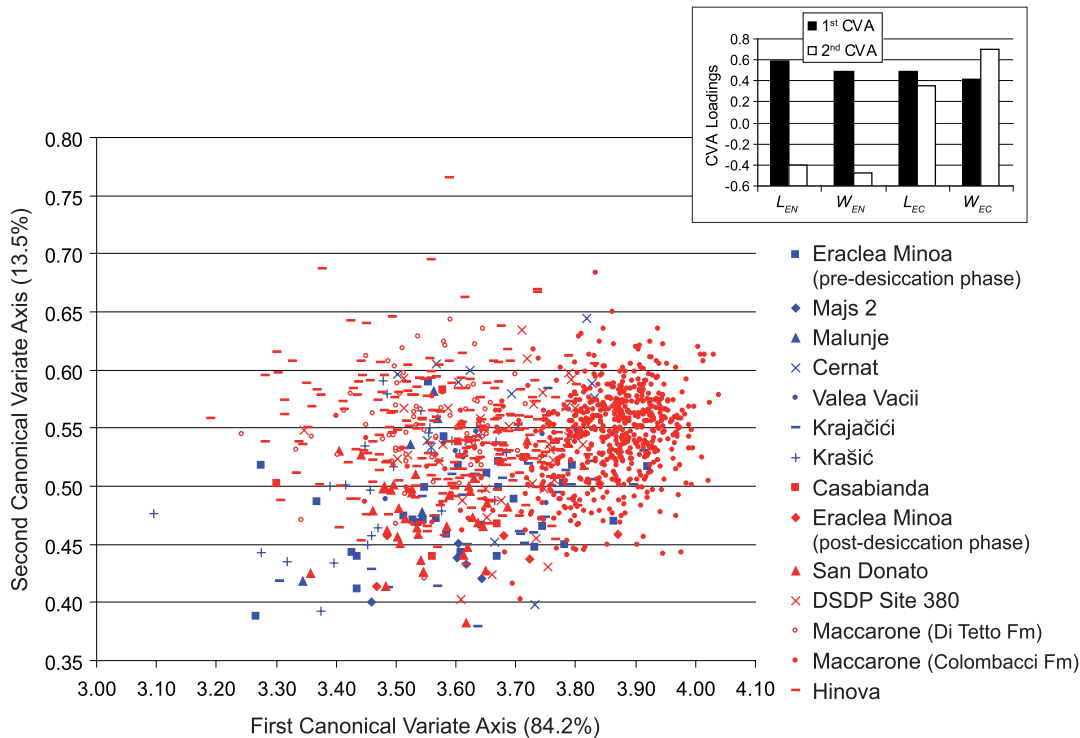
separation, i.e. the smaller the endocyst with respect to the ectocyst, the smaller  $Y$  and  $D_{EN/EC}$ . Thus, it is an estimate of one of the main 'shape parameters' classically used to describe and discriminate the dinoflagellate cyst taxa considered in this work (see Introduction).

We then further analyzed each sampled  $Y$ -distribution for multi-normality using mixture analysis (Redner and Walker, 1984; Titterton et al., 1985). In each case, the mixture with the lowest associated Akaike Information Criterion value was selected in order to favour the solution that produces the best fit without overfitting.

Most comparisons were achieved using Student's  $t$ -tests and one-way analyses of variance (ANOVA), including in both cases a Welch–Satterthwaite correction for unequal variances between samples when necessary (Satterthwaite, 1946; Welch, 1947; Sokal and Rohlf, 1995). All statistical analyses were performed using the PAST software, v. 1.64 (Hammer et al., 2001).

## RESULTS

$X$  and  $Y$  distributions were first analyzed for the two most intensively sampled lower Zanclean sections: Maccarone (13 samples, 698 individuals) and Hinova (16 samples, 247 individuals) (Text-Figure 6). One-way ANOVAs of  $X$  and  $Y$  indicate a very high inter-level heterogeneity for both descriptors in the Maccarone section ( $X$ :  $F = 87.9$ ;  $d.f. = 12, 97$ ;  $p = 2 \times 10^{-46}$ ;  $Y$ :  $F = 13.9$ ;  $d.f. = 12, 99$ ;  $p = 2 \times 10^{-16}$  [both ANOVAs include a Welch–Satterthwaite correction]). Conversely, no heterogeneity is found in the Hinova section ( $X$ :  $F = 1.15$ ;  $d.f. = 15, 231$ ;  $p = 0.31$ ;  $Y$ :  $F = 1.04$ ;  $d.f. = 15, 231$ ;  $p = 0.41$ ). After the Messinian Salinity Crisis, no significant changes thus appear at Hinova in the size and shape of *Galeacysta etrusca*, with individuals showing a mean  $D_{EN/EC}$  ratio of about 35%. In contrast, a three-step sequence is evidenced at Maccarone. At the beginning of the analyzed series of samples (levels 15 to 18: Popescu et al., 2007), assemblages comprise rather small-sized individuals with a mean  $D_{EN/EC}$  ratio of about 34%, identical at the 95% confidence level to that observed at Hinova (Student's  $t$ -test:  $t = 1.87$ ;  $d.f. = 323$ ;  $p = 0.063$ ). At the end of the sequence (samples 35 to 42: Popescu et al., 2007), assemblages comprise rather large individuals with a mean  $D_{EN/EC}$  ratio of about 41%, both  $X$  and  $Y$  mean values being significantly greater than observed previously (Student's  $t$ -test on  $X$ :  $t = 28.6$ ,  $d.f. = 564$ ,  $p = 3 \times 10^{-47}$ ; Student's  $t$ -test on  $Y$ :  $t = 7.14$ ,  $d.f. = 564$ ,  $p = 3 \times 10^{-12}$ ). Between these two sets of assemblages, intermediate samples illustrate a gradual compositional transition from assemblages dominated by small individuals with a mean  $D_{EN/EC}$  ratio close to 34%, to assemblages dominated by large-sized individuals with a mean  $D_{EN/EC}$  ratio of about 41%. Hence, the 'transition



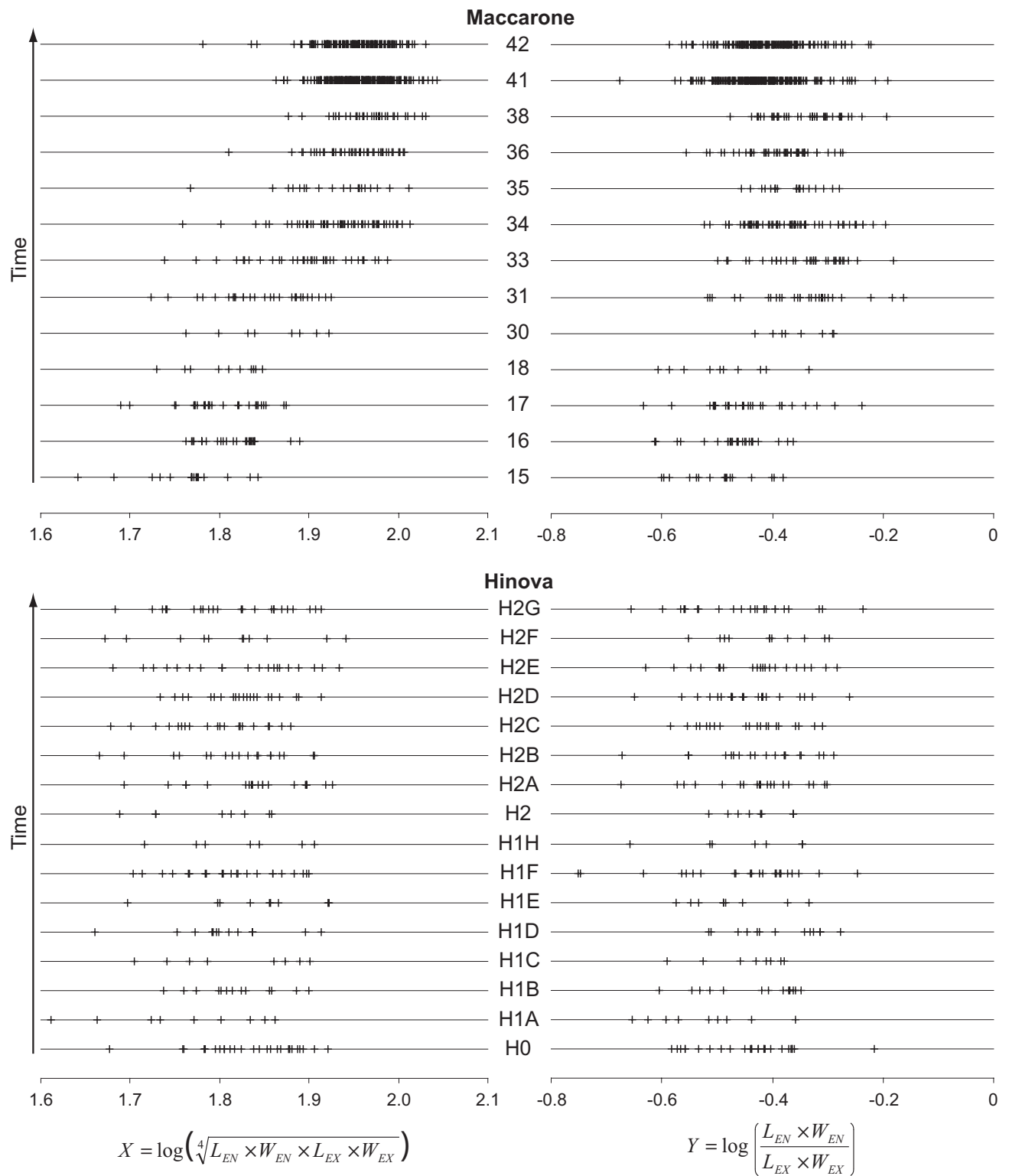
Text-Figure 5. First canonical plane resulting from a one-way Multiple Analysis of Variance based on the four log-transformed initial variables: length and width of the endocyst (noted  $L_{EN}$  and  $W_{EN}$ , respectively) and length and width of the ectocyst (noted  $L_{EC}$  and  $W_{EC}$ , respectively). MANOVA's highly significant results (Wilk's  $\lambda = 0.455$ ;  $d.f. = 48, 4347$ ;  $F = 20.5$ ,  $p = 5 \times 10^{-156}$ ) allow the identification of two main sources of biometric variation: overall dinoflagellate cyst size on the first canonical variate axis, and  $D_{ENIEC}$  ratio on the second canonical variate axis (inset; see text for details).

effect' observed between the lower and upper parts of the Maccarone section is not the result of a gradual biometric change of individuals, but is the simple consequence of the gradual changing in relative abundance of smaller-sized and smaller- $D_{ENIEC}$  individuals (characteristic of the lower part of the analyzed time series) and larger-sized and larger- $D_{ENIEC}$  individuals (characteristic of the upper part of the analyzed section). Thus, these first results clearly indicate that at least two stable, dimensionally homogeneous biometric groups (hereafter named 'groups') with mean  $D_{ENIEC}$  ratios of about 34% and 41%, respectively, can be statistically distinguished at Maccarone, whereas a single one is evidenced throughout the Hinova section.

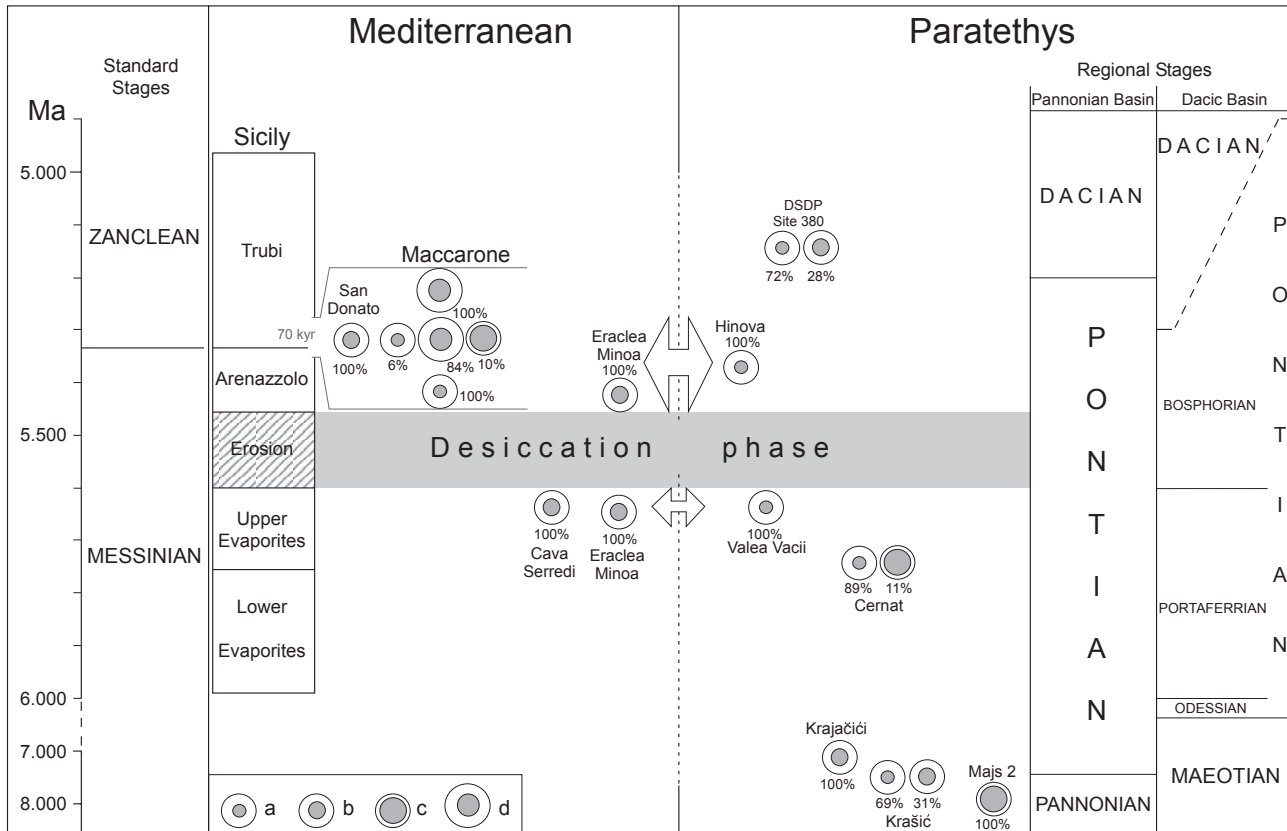
At the level of the complete analyzed data set, mixture analyses of the 39 sampled  $Y$ -distributions allowed us to identify four distinct stable biometric groups (named 'a' to 'd'; Plate 2) although these partly overlap one another (Table 2; Text-Figure 7). Groups 'a', 'b' and 'c' are characterized by individuals with a small, intermediate, and large  $D_{ENIEC}$  ratio, with mean values of ca. 32–36%, 47–53%, and 60%, respectively, inversely related to the relative distance between the endocyst and ectocyst – the

greater the  $D_{ENIEC}$ , the smaller the distance. These three groups do not differ from one another in their mean size ( $X$ ) values (see below). In contrast, group 'd' is characterized by large individuals with a  $D_{ENIEC}$  ratio of ca. 39–43%, intermediate between the mean values of groups 'a' and 'b'. Individuals from the previously described assemblages of the Hinova section and the lower part of the Maccarone section are referred to group 'a', while those of the upper part of the Maccarone section belong to group 'd'.

In several localities, only one of the four biometric groups occurs (e.g. Valea Vacii and Hinova for group 'a', Krajačići and Eraclea Minoa for group 'b', Majs 2 for group 'c', and Maccarone samples 35 to 42 (Popescu et al., 2007) for group 'd'), allowing us to draw an  $XY$  scatter plot for the corresponding individuals (Table 2; Text-Figure 8). A small but highly significant positive linear relationship between  $X$  and  $Y$  is observed only for group 'a' ( $R^2 = 0.081$ ,  $n = 333$ ,  $p_{[H_0: R^2=0]} = 1.3 \times 10^{-7}$ ), whereas for both groups 'b' and 'd',  $X$  and  $Y$  appear linearly independent ('b':  $R^2 = 1.6 \times 10^{-3}$ ,  $n = 107$ ,  $p = 0.68$ ; 'd':  $R^2 = 2.4 \times 10^{-3}$ ,  $n = 482$ ,  $p = 0.29$ ). From this perspective, group 'd', which is observed only in the upper part of the Maccarone section (samples 35



Text-Figure 6. Evolution of  $X$  (the dinoflagellate cyst log-transformed geometric mean size) and  $Y$  (the dinoflagellate cyst log-transformed  $D_{EN/EC}$  ratio) distributed through the early Zanclean at the Maccarone (694 individuals) and Hinova sections (248 individuals). The Maccarone samples are from Popsecu et al. (2007), and the Hinova samples are from Popescu (2001).



Text-Figure 7. Distribution of the *Galeacysta etrusca* biometric groups recorded in the studied localities with their respective percentages. Legend as for Text-Figure 2. The time interval encompassing the Colombacci Formation in the Apennine foredeep (Maccarone and San Donato sections) is enlarged. Groups: 'a', small individuals with small (ca. 32–36%)  $D_{ENIEC}$  ratio; 'b', small individuals with intermediate (ca. 47–53%)  $D_{ENIEC}$  ratio; 'c', small individuals with large (ca. 60%)  $D_{ENIEC}$  ratio; 'd', large individuals with small to intermediate (ca. 39–43%)  $D_{ENIEC}$  ratio.

to 42: Popescu et al., 2007), can be regarded as a local adaptation directly replacing group 'a' (samples 15 to 18: Popescu et al., 2007). Actually, group 'd' is characterized by  $X$ -values noticeably (ca. 30%) greater than the three other groups, indicating larger individuals, and  $Y$ -values

slightly larger than for group 'a'. Conversely, groups 'a' and 'b' (and also 'c') cannot be distinguished based on  $X$ -values, but can be statistically identified based on  $Y$ . A one-way ANOVA of  $Y$  between groups 'a', 'b' and 'd' (group 'c' is not considered due to its scarcity in the data set)

## PLATE 2

Scanning electron photomicrographs of specimens of the *Galeacysta etrusca* complex. Specimens are assigned to morphological groups as defined in this study using biometric analysis. The scale bar represents 20  $\mu\text{m}$ .

- 1 Group 'a' specimen from Hinova (Dacic Basin), sample H2.
- 2 Group 'a' specimen from Hinova (Dacic Basin), sample H2.
- 3 Group 'a' specimen from Krašić (Pannonian Basin), sample I 1/1.
- 4 Group 'a' specimen from Maccarone (central Italy), sample 33.
- 5 Group 'a' specimen from Maccarone (central Italy), sample 33.
- 6 Group 'b' specimen from Krajačići (Pannonian Basin), sample I 1/1.
- 7 Group 'b' specimen from DSDP Site 380 (Black Sea), sample 828.02 m depth.
- 8 Group 'c' specimen from Majs 2 (Pannonian Basin), sample 257.30 m depth.
- 9 Group 'c' specimen from Majs 2 (Pannonian Basin), sample 257.30 m depth.
- 10 Group 'd' specimen from Maccarone (central Italy), sample 42.
- 11 Group 'd' specimen from Maccarone (central Italy), sample 42.
- 12 Group 'd' specimen from Maccarone (central Italy), sample 42.

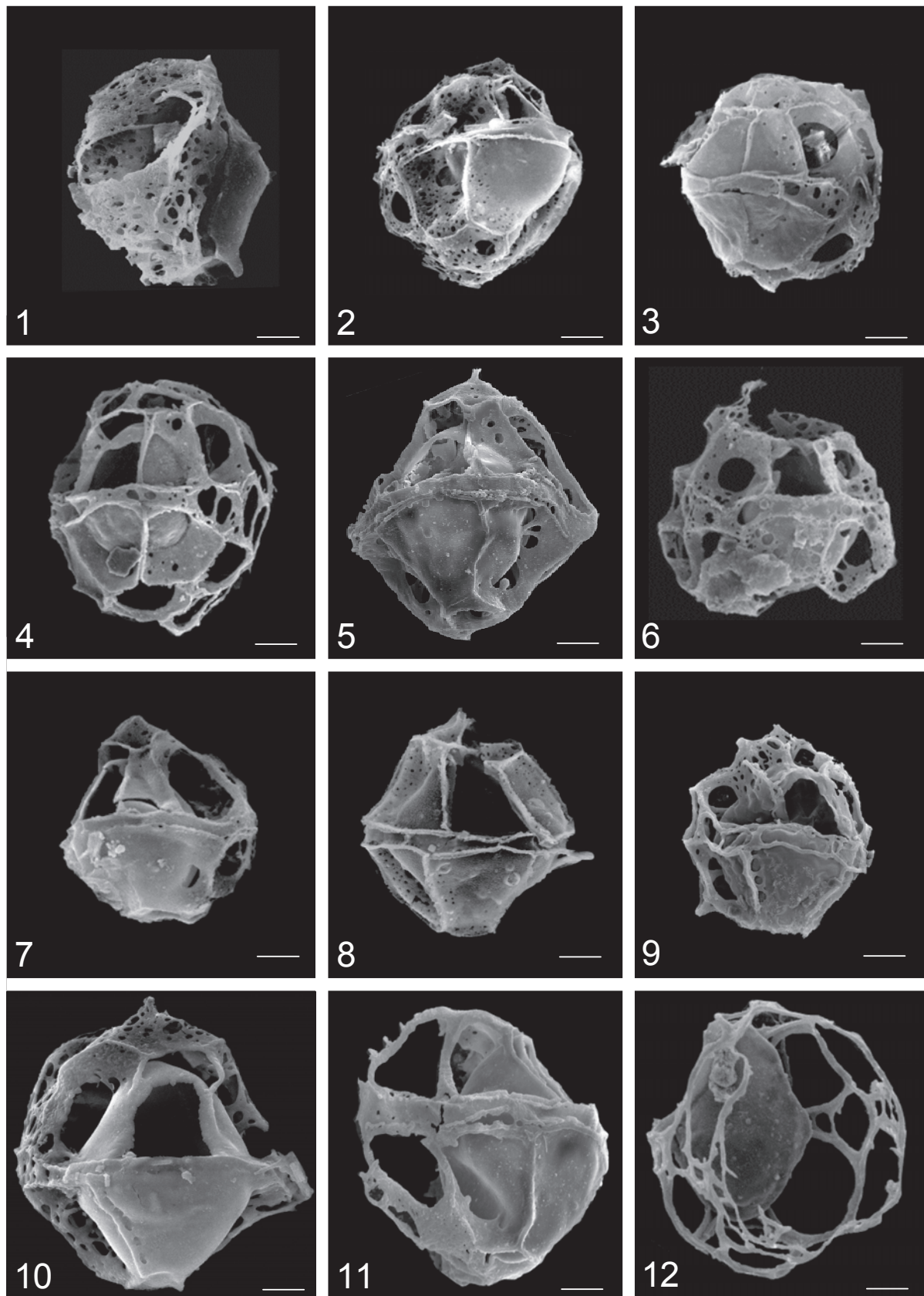
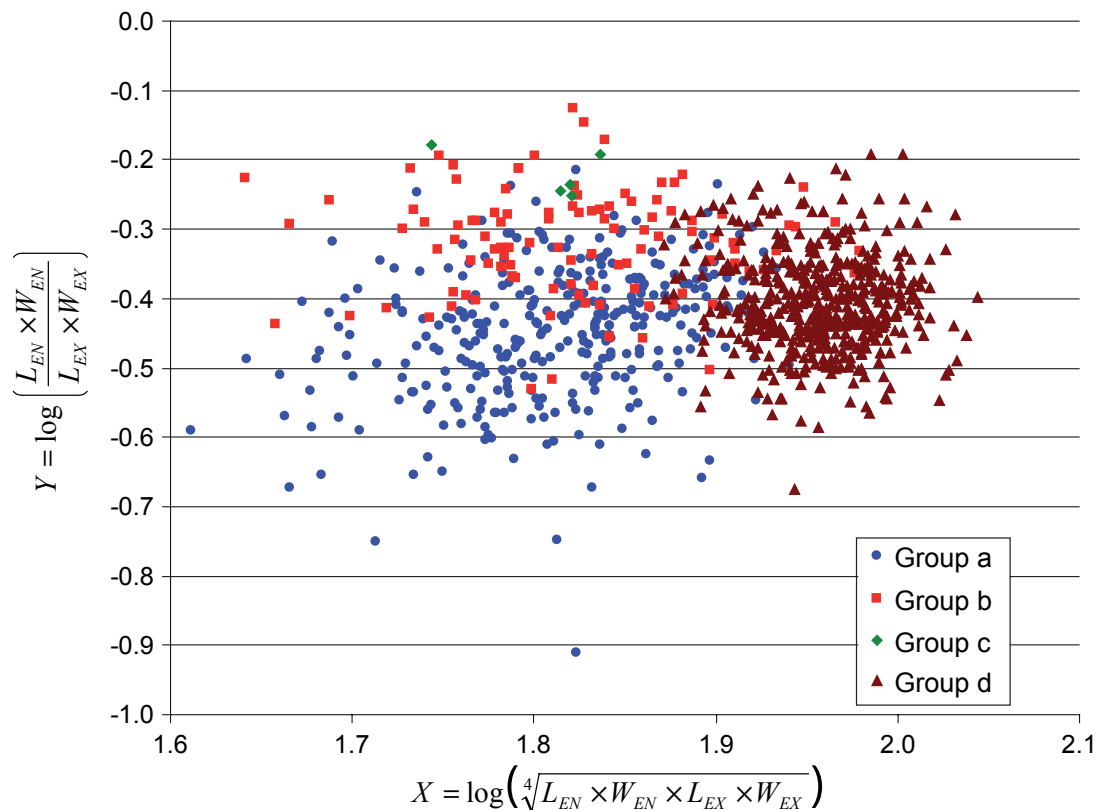


Table 2. Mixture analysis results of the 38 sampled distributions of the dinoflagellate cyst shape parameter:  $Y = \log\left(\frac{L_{EN} \times W_{EN}}{L_{EC} \times W_{EC}}\right)$ .

$N$ : sample size;  $\mu \pm \sigma$ , %:  $Y$  mean  $\pm$  standard deviation; and relative abundance of the identified biometric groups.

Sample	$N$	Group a		Group b		Group c		Group d	
		$\mu \pm \sigma$	%						
Eraclea Minoa (lower)	30	—	—	-0.324±0.069	100	—	—	—	—
Majs 2	5	—	—	—	—	-0.221±0.030	100	—	—
Cernat	18	-0.478±0.062	89	—	—	-0.212±0.042	11	—	—
Valea Vacci	8	-0.396±0.040	100	—	—	—	—	—	—
Krajačiči	27	—	—	-0.317±0.073	100	—	—	—	—
Krašić	26	-0.434±0.061	69	-0.277±0.032	31	—	—	—	—
Eraclea Minoa (upper)	7	—	—	-0.275±0.069	100	—	—	—	—
San Donato	37	—	—	-0.308±0.070	100	—	—	—	—
DSDP Site 380	33	-0.452±0.069	72	-0.287±0.066	28	—	—	—	—
Hinova – H0	26	-0.444±0.084	100	—	—	—	—	—	—
Hinova – H1A	9	-0.426±0.089	100	—	—	—	—	—	—
Hinova – H1B	13	-0.438±0.083	100	—	—	—	—	—	—
Hinova – H1C	8	-0.447±0.070	100	—	—	—	—	—	—
Hinova – H1D	13	-0.391±0.006	100	—	—	—	—	—	—
Hinova – H1E	9	-0.475±0.074	100	—	—	—	—	—	—
Hinova – H1F	22	-0.463±0.126	100	—	—	—	—	—	—
Hinova – H1H	7	-0.459±0.102	100	—	—	—	—	—	—
Hinova – H2	8	-0.433±0.050	100	—	—	—	—	—	—
Hinova – H2A	19	-0.434±0.096	100	—	—	—	—	—	—
Hinova – H2B	18	-0.428±0.095	100	—	—	—	—	—	—
Hinova – H2C	20	-0.446±0.078	100	—	—	—	—	—	—
Hinova – H2D	21	-0.444±0.085	100	—	—	—	—	—	—
Hinova – H2E	20	-0.433±0.091	100	—	—	—	—	—	—
Hinova – H2F	11	-0.413±0.078	100	—	—	—	—	—	—
Hinova – H2G	23	-0.451±0.099	100	—	—	—	—	—	—
Maccarone – 15	16	-0.496±0.067	100	—	—	—	—	—	—
Maccarone – 16	24	-0.474±0.063	100	—	—	—	—	—	—
Maccarone – 17	29	-0.438±0.082	100	—	—	—	—	—	—
Maccarone – 18	10	-0.488±0.081	100	—	—	—	—	—	—
Maccarone – 30	8	—	—	—	—	—	—	-0.354±0.050	100
Maccarone – 31	27	-0.494±0.025	18	—	—	-0.188±0.024	11	-0.341±0.041	71
Maccarone – 33	36	-0.487±0.008	7	—	—	—	—	-0.334±0.061	93
Maccarone – 34	59	—	—	—	—	-0.253±0.030	18	-0.399±0.055	82
Maccarone – 35	19	—	—	—	—	—	—	-0.368±0.048	100
Maccarone – 36	44	—	—	—	—	—	—	-0.390±0.064	100
Maccarone – 38	35	—	—	—	—	—	—	-0.344±0.064	100
Maccarone – 41	236	—	—	—	—	—	—	-0.421±0.066	100
Maccarone – 42	155	—	—	—	—	—	—	-0.409±0.066	100



Text-Figure 8. XY scatter plot of the single-group samples (see Table 2 and explanations in the text).

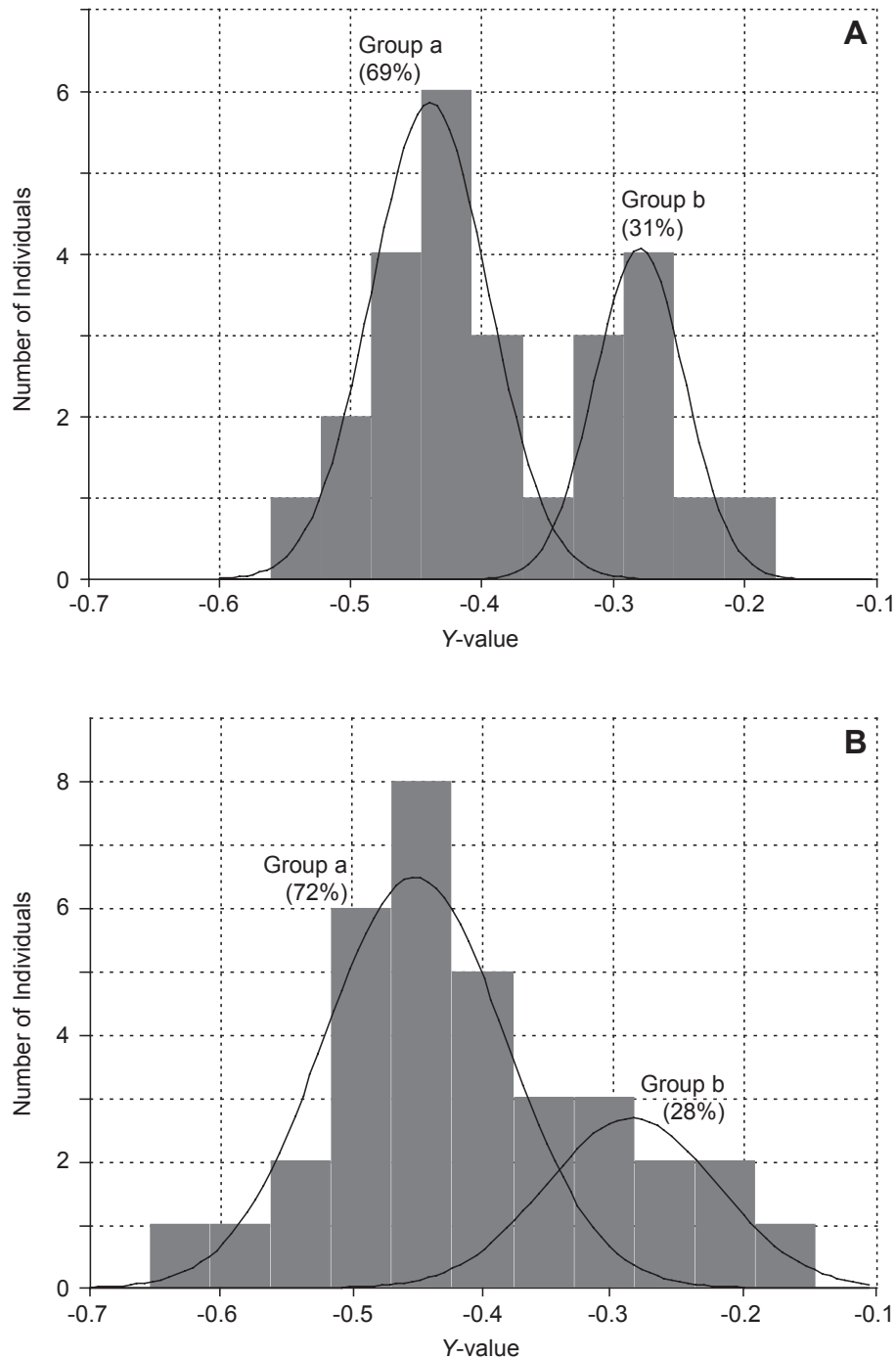
indicates a highly significant global heterogeneity between the three groups:  $F = 102.5$ ,  $d.f. = 2, 284$ ;  $p = 3 \times 10^{-34}$  (including a Welch–Satterthwaite correction). A post-hoc contrast analysis, using Tukey’s HSD test, returns highly significant  $p$ -values for all three couples of groups ([a-b], [a-d] and [b-d]:  $p = 2.2 \times 10^{-5}$  in all three cases), indicating significant pairwise differences between the three groups.

In some samples, two biometric groups occur together (e.g. Krašić and DSDP Site 380 for groups ‘a’ and ‘b’, Cernat for groups ‘a’ and ‘c’). The way groups ‘a’ and ‘b’ are identified in such mixed samples is exemplified in Text-Figure 9. These two examples show that when these two groups are found simultaneously, their  $Y$  distribution partially overlaps. This first indicates that the rather large amount of superposition of groups ‘a’ and ‘b’ in Text-Figure 9 is partially, but very likely not completely, ‘real’. It could actually be, at least partially, an artificial consequence of failure of the mixture analysis to detect the joint occurrence of these two groups, leading to a false identification of individuals from group ‘b’ as belonging to group ‘a’ (or vice versa) when one of them markedly dominates the sample assemblage. Second, both Text-Figures 8 and 9 thus reveal that these biometric groups can only be identi-

fied and distinguished by statistical means, and by no means correspond to discrete morphotypes referable to distinct dinoflagellate cyst species. Statistically different stable biometric variants of *Galeacysta etrusca* do exist, but these variants describe a morphological continuum with no clear limits between them.

In summary, the following observations can thus be made (Table 2; Text-Figure 7). Prior to the Messinian Salinity Crisis, group ‘b’ is recorded alone at Krajačići (Plate 2, fig. 6), and group ‘c’ at Majs 2 (Plate 2, figs. 8, 9). At Krašić (Plate 2, fig. 3), group ‘a’ is prevalent but group ‘b’ is significantly represented. Groups ‘a’ and ‘c’ are unequally represented at Cernat, and group ‘a’ alone has been recorded at Valea Vacii. The *Galeacysta etrusca* specimens represented in the Mediterranean Basin as recorded at Cava Serredi and Eraclea Minoa belong to group ‘b’.

After the Messinian Salinity Crisis, the *Galeacysta etrusca* assemblage from Hinova (Plate 2, figs. 1, 2) comprises only specimens of group ‘a’, but that from DSDP Site 380 is represented by groups ‘a’ (dominant) and ‘b’ (Plate 2, fig. 7). Specimens recorded at Eraclea Minoa belong entirely to group ‘b’. Assemblages from Maccarone are more diverse



Text-Figure 9. Y-distribution histograms of *Galeacysta etrusca* complex assemblages showing Gaussian distributions superimposed for groups 'a' and 'b' (see Table 2 for the numerical values of estimated distribution parameters). Assemblages from: **A)** Krašić (Messinian); and **B)** DSDP Site 380 (Zanclean).

and have changed along the interval during which *Galeacysta etrusca* is recorded: at the beginning of invasion, only group 'a' (Plate 2, fig. 4) is present; then, three groups are recorded at the same levels (mostly group 'd', with 'a' and 'c' as

subordinate groups); and finally only group 'd' remains (Plate 2, figs. 10–12). At San Donato, the *Galeacysta etrusca* specimens measured within the interval preceding its disappearance belong exclusively to group 'b'.

## DISCUSSION

### Paratethyan and Mediterranean *Galeacysta etrusca* History Around the Messinian/Zanclean Boundary

In this study, the oldest *Galeacysta etrusca* specimens are of late Pannonian age (the Majs 2 section in the Pannonian Basin) and belong to biometric group 'c', i.e. specimens with rather high  $D_{EN/EC}$  ratios corresponding to relatively small distances between endocyst and ectocyst (Plate 2, figs. 8, 9). Within this basin, we then distinguish groups 'a' and 'b' in the latest Pannonian Krašić section (Plate 2, fig. 3) and group 'b' in the Krajačići section (Plate 2, fig. 6). Differences between these assemblages cannot be explained by time alone but, more probably, by an already existing paleoenvironmental diversification within the Pannonian Basin. The exclusive occurrence of group 'c' at Majs 2, although based only on five specimens (Table 2), suggests that *Galeacysta etrusca* specimens were living in fresh to brackish conditions just before the marine connection between the Pannonian Basin and the Mediterranean Sea (see above). This assumption is in agreement with the absence of other marine organisms (including other dinoflagellate cyst species) and is consistent with the high  $D_{EN/EC}$  ratio of *Galeacysta etrusca*. Groups 'a' and 'b' identified at the Krašić and Krajačići sections (Plate 2, figs. 3, 6) show decreases in their  $D_{EN/EC}$  ratio, probably in response to increased salinity as a result of the connection at high-sea level between the Pannonian Basin and Mediterranean Sea. This connection is supported by the presence in the Pannonian sections of Mediterranean calcareous nannoplankton and marine dinoflagellate cysts (*Achomosphaera andalousiensis*, *Nematosphaeropsis labyrinthus*) as at Krajačići.

For the Dacic Basin, at Cernat, analyses show two biometric groups: (1) group 'c', characterized by a high  $D_{EN/EC}$  ratio, is represented in low percentages (11%) and corresponds to the 'old' Pannonian stock, and (2) group 'a', which is dominant (89%) and could be related to more saline conditions than those associated with group 'c', induced by the connection between the Dacic Basin and Mediterranean Sea during the Portaferrian–Bosphorion, as indicated by recognition of the NN11b calcareous nannoplankton subzone in the same samples. The exclusive persistence of group 'a' in the early Bosphorion Valea Vacii section suggests that environmental conditions in the Dacic Basin were stable and more saline in the early Bosphorion than in the Portaferrian.

Before the Messinian Salinity Crisis, the southwestern Euxinian Basin was characterized by freshwater conditions based on Schrader's (1978) diatom record at DSDP Site 380 (Text-Figure 1). Indeed, we found no marine or brack-

ish dinoflagellate cysts, including *Galeacysta etrusca*, in the same intervals of DSDP Site 380 (Popescu, 2006). However, the presence in the Crimea of calcareous nannoplankton of subzone NN11b (Semenenko and Olejnik, 1995) indicates that the Euxinian and Dacic basins were probably connected in the early Bosphorion. The gateway was located at the Reni Strait according to Semenenko and Olejnik (1995).

In the Mediterranean Basin, only *Galeacysta etrusca* group 'b' was recorded at Cava Serredi and Eraclea Minoa, in deposits dating from the latest Messinian. At Cava Serredi, *Galeacysta etrusca* sensu stricto is accompanied by *Impagidinium* sp. 1 and 2 of Corradini and Biffi (1988), which may be referable to *Millioudodinium bacculatum* and *Spiniferites cruciformis*, respectively (Popescu et al., 2007), two species with Paratethyan affinities. Group 'b' recorded in the Mediterranean Basin probably represents an adaptation of *Galeacysta etrusca* to a new environment after its arrival from the Paratethys during the high sea-level just preceding the peak of the Messinian Salinity Crisis (i.e. the desiccation phase delimited in Text-Figure 7). Group 'a' has a lower  $D_{EN/EC}$  ratio than group 'b', but as shown above, these groups can occur simultaneously and do not correspond to clearly discrete morphotypes. The presence of *Galeacysta etrusca* in the Mediterranean Basin before the Messinian Salinity Crisis peak documents the connection between the Mediterranean and Paratethys in the late Messinian corresponding to the first 'Lago Mare' event (Clauzon et al., 2005).

Connections between the remnant Paratethys and the Mediterranean between 8 and 5 Ma are debated intensely, as are the connections between the Paratethyan basins themselves (Stevanović, 1974; Archambault-Guézou, 1976; Rögl and Steininger, 1983; Kojumdgieva, 1987; Marinescu, 1992; Magyar et al., 1999b; Müller et al., 1999; Meulenkamp and Sissingh, 2003; Popov et al., 2006; and Piller et al., 2007). Based on the evidence of similar fossils (mainly *Congerina rhomboidea*) in the Pannonian and Dacic basins, Stevanović (1951) proposed the opening of a gateway between these basins in the area of the Iron Gates, and created the Portaferrian Regional Substage (from the French *Portes de Fer* for Iron Gates). In fact, the Portaferrian Substage sensu Stevanović (1951) corresponds partly to the upper part of the Pannonian Stage in the Lake Pannon (Magyar et al., 1999a; Müller et al., 1999; Piller et al., 2007), the waters of which temporarily entered the Dacic Basin.

The presence of Mediterranean calcareous nannoplankton in the Maeotian of the Dacic Basin (Mărunțeanu and Papaianopol, 1998; Snel et al., 2006) and also the Pannonian Basin at Krajačići, simultaneously with the presence of Mediterranean marine dinoflagellate cysts,

suggests that these Paratethyan basins were independently connected to the Mediterranean Sea at high sea-level at around 7 Ma. It has been demonstrated that the Iron Gates passage through the Carpathians, constantly refuted by Marinescu (1992), was in fact made by fluvial downcutting during the peak of the Messinian Salinity Crisis (Clauzon et al., 2005; Leever, 2007). In addition, it has been established by Clauzon et al. (2005) that the connection between the Dacic Basin and the Mediterranean Sea, passing through Thessaloniki, Skopje, Niš and the modern Timok Valley (Text-Figure 10A, B), was probably active from 13.5 Ma until about 4 Ma based on the occurrence of Mediterranean calcareous nannoplankton in the Dacic Basin (Mărunțeanu and Papaionopol, 1995; 1998). As a consequence, we propose that this corridor extended through a western branch entering the Pannonian Basin in the area of Niš–Belgrade up to 5.60 Ma exclusively (Text-Figure 10A). As the western branch of this corridor was probably already active at about 7 Ma, based on the marine dinoflagellate cysts and nannoplankton recorded at Krajačići (Text-Figure 2), one must envisage some delay in the arrival of the sublittoral to lacustrine *Congerina rhomboidea* in the Dacic Basin. In any case, all the data are in agreement with the closure of this branch at the beginning of the Bosphorion (Text-Figure 2). A two-way current probably worked in such gateways, as today in the Bosphorus Strait where marine Mediterranean water inflows through the corridor as bottom water, where it brings marine organisms to the Black Sea, while less saline Black Sea water outflows at the surface and transports brackish organisms into the Mediterranean (Guibout, 1987; Bethoux and Gentili, 1999). Such similar opposed currents may have existed in the past and explain the repeated entries of *Galeacysta etrusca* into the Mediterranean Basin.

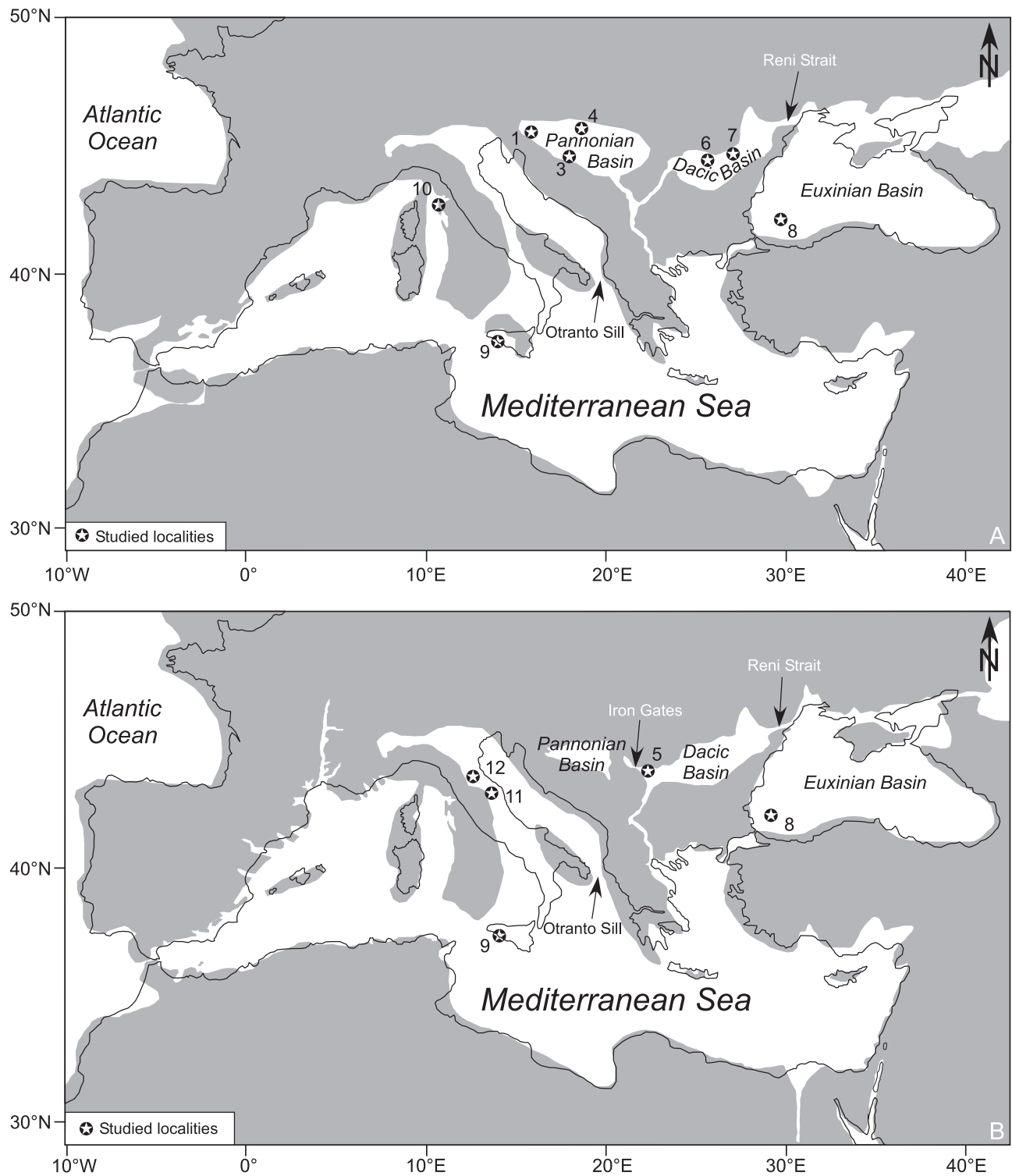
During the Messinian Salinity Crisis, important paleogeographic changes impacted Europe: the Mediterranean and Black Sea (i.e. the Euxinian Basin) almost desiccated; the Dacic Basin, the Adriatic and Po realm persisted as suspended lakes (Clauzon et al., 2005, Popescu et al., 2007) and became brackish to freshwater; and the Pannonian Basin became very reduced as it was also affected by intense fluvial erosion (Csato et al., 2007).

*Galeacysta etrusca* group 'a' (Plate 2, figs. 1, 2), having been prevalent in the Dacic Basin before the peak of the Messinian Salinity Crisis, probably survived when this basin partly contracted as a suspended lake during the paroxysm of the crisis (Clauzon et al., 2005). Consequently, it was alone in the basin during the earliest Zanclean (Hinova section). As soon as the connection between the Dacic Basin and the Mediterranean Sea was re-established at the end of the Messinian Salinity Crisis, this species re-

invaded the Mediterranean realm. At that time, group 'b', which replaces group 'a' when salinity increases, is recorded at Eraclea Minoa in fully marine waters accompanied by the other Paratethyan species *Spiniferites cruciformis*, *Pterocysta cruciformis*, and *Seriliodinium explicatum* (Londeix et al., 2007).

Fresh- to brackish-water conditions existed in the Adriatic–Po realm in the latest Messinian as indicated at the Maccarone section (Popescu et al., 2007). But Popescu et al. (2007, fig. 7) have shown that two major marine incursions were recorded at Maccarone: (1) below the Colombacci Formation (i.e. the second 'Lago Mare' event) as supported by abundant marine dinoflagellate cysts and a high diversity of calcareous nannoplankton including the marker *Ceratolithus acutus* (Text-Figure 2), and (2) above the Colombacci Formation as supported by such marine organisms as dinoflagellate cysts, calcareous nannoplankton and more abundant planktonic foraminifers. The first marine incursion probably changed the existing freshwater conditions into brackish water ones, similar to those of the Dacic Basin, and thus permitting the immigrant Paratethyan species to colonize this basin without changing their morphology. Indeed, *Galeacysta etrusca* was first represented by group 'a' (Plate 2, figs. 4, 5; Text-Figure 7). Then, continuous freshwater river input and brief minor marine influxes within the Colombacci Formation induced weak fluctuations in salinity and nutrients that might explain the morphological diversification of *Galeacysta etrusca* into groups 'c' and 'd' while accompanied by the persisting group 'a' (Plate 2, figs. 4, 5, 10–12; Text-Figures 6, 7). Finally, the development of stable environmental conditions produced group 'd' in the uppermost Colombacci Formation before its disappearance at the second major marine invasion (Plate 2, figs. 10–12; Text-Figure 7). With respect to the recent chronology established for the Maccarone section (Popescu et al., 2007), this adaptation process lasted only about 70 kyr, i.e. between the first appearance of *Ceratolithus acutus* (5.345 Ma: Raffi et al., 2006) and a little later than the disappearance of *Triquetrorhabdulus rugosus* (5.279 Ma: Raffi et al., 2006). Northward, at San Donato (Text-Figure 1), *Galeacysta etrusca* arrived later (in the uppermost layer of the Colombacci Formation) without other Paratethyan immigrants, when marine conditions were almost completely established. This explains why group 'b' alone is recorded, as at Eraclea Minoa.

Later, at ca. 5.13 Ma, dinoflagellates of the Dacic Basin entered the Black Sea (Euxinian Basin) when the sea level rose to overflow the sill that presumably existed at the Reni Strait, developing predominant cysts of group 'a' accompanied by fewer specimens of group 'b' (Plate 2, fig. 7).



Text-Figure 10. Paleogeography of the Mediterranean and central–eastern Paratethys (land areas in gray) based on Popov et al. (2006) but revised in accordance with our observations and deductions. **A)** Late Messinian, before the peak of the Messinian Salinity Crisis. **B)** Latest Messinian–Early Zanclean, after the peak of the Messinian Salinity Crisis. Corresponding studied localities with specimens of the *Galeacysta etrusca* complex are shown: 1, Krašić; 3, Krajačići; 4, Majs 2; 5, Hinova; 6, Cernat; 7, Valea Vacii; 8, DSDP Site 380; 9, Eraclea Minoa; 10, Cava Serredi; 11, Maccarone; and 12, San Donato.

### Environmental, Hydrographic and Geographic Insights from *Galeacysta etrusca*

Based on the above scenario, it is now possible to address the questions proposed in the Introduction.

First, it appears unrealistic to distinguish from available evidence the two ‘Lago Mare’ events in the Mediterranean Basin on the basis of *Galeacysta etrusca* biometry as we have measured it. Indeed, this study establishes that each invasion of Paratethyan dinoflagellates is represented by *Galeacysta etrusca* individuals exclusively belonging to biometric group ‘a’ (corresponding to specimens with a relatively large separation between the endocyst and ectocyst), which probably reflects a stable morphology related to more saline conditions, as found in the Paratethyan sections and in the lower part of the studied Maccarone section. When the species faces marine conditions, group ‘a’ is replaced by group ‘b’, as recorded at Cava Serredi and Eraclea Minoa. Group ‘d’ seems to be linked to increases both in salinity and nutrient content. Finally, group ‘c’ appears to characterize freshwater environments.

Second, the high environmental sensitivity of *Galeacysta etrusca*, combined with the precise and reliable chronology of the materials studied, undoubtedly refine our knowledge of the Central–Eastern Mediterranean and Paratethys during the interval 6–5 Ma, as detailed below.

From ca. 8 Ma to 5.60 Ma (Text-Figures 2, 7), the connection between the Pannonian Basin and both the Dacic Basin and the Mediterranean Sea should be envisaged as a Y-shaped corridor with two northern branches diverging northward of Niš (Text-Figure 10A). This reconstruction is consistent with geological maps (Kräutner and Krstić, 2003) and some previous assumptions (see, for example, Stanković *in* Hsü et al., 1978, p. 1073, except that we attribute the ‘Lago Mare’ events to exchanges at high sea-level between the Mediterranean and Paratethys; see also Marinescu *in* Hsü, 1978, p. 517, except that their map was proposed for the Pliocene and shows a different passage at the place of the Iron Gates, a possibility quite rightly refuted by Marinescu, 1992). The gateway proposed here not only allowed Pannonian Basin–Mediterranean and Dacic Basin–Mediterranean exchanges but also Pannonian–Dacic basin exchanges. Southward, this corridor passed through Skopje to reach the Aegean Sea at the present-day Gulf of Thermaikos (Clauzon et al., 2005). Along this corridor (Text-Figure 10A) we observe several Upper Miocene and Zanclean Mediterranean marine deposits separated by a strong erosional surface (Clauzon et al., 2008). After the Messinian Salinity Crisis, the corridor was re-established without its western branch, probably because of

uplift in the southwestern Carpathians. Water-mass exchanges at high sea-level resumed, but were limited to the Mediterranean and the Dacic Basin while the Pannonian Basin was isolated and significantly restricted (Text-Figure 10B). The corridor probably joined the Dacic Basin in the area of the present-day Timok Valley, i.e. at the distal part of the Zanclean Gilbert-type fan delta constructed by the proto-Danube River, which cut the Carpathians during the Messinian desiccation phase at the place of the present-day Iron Gates Gorge (Text-Figure 10B; Clauzon et al., 2005; Leever, 2007). This proto-Danube River probably originated at the western edge of the Carpathians, where some important latest Miocene fluvial erosion is evident (Csato et al., 2007).

The late arrival of Mediterranean dinoflagellate cysts in the southern Black Sea requires explanation. Because the Black Sea desiccated at the same time as the Mediterranean, one must consider: (1) a connection with the Mediterranean Sea prior to the Messinian Salinity Crisis, and (2) the emerging regionally drier climatic conditions evidenced by Popescu (2006), which were likely reinforced considerably by the Mediterranean desiccation in progress. It has been demonstrated that no connection was possible through the area of the present-day Bosphorus Strait before or after the crisis (Popescu, 2006), an assumption reinforced by evidence of the Messinian Erosional Surface at DSDP Sites 381 and 380, i.e. extending from the southwestern Black Sea shelf to the basin (Gillet et al., 2007). Hence, the connection between the Black Sea and the Mediterranean seems to have been through the Dacic Basin and the Reni Strait in the area of the Dobrogea horst, as proposed by Semenenko and Olejnik (1995). No Mediterranean calcareous nannoplankton were recorded at DSDP Site 380 before the crisis, and no Mediterranean dinoflagellate cysts were found before the crisis although they invaded this basin after a delay of 200 kyr in the early Zanclean. However, Mediterranean marine calcareous nannoplankton arrived at the Crimea before and after the Messinian Salinity Crisis (subzones NN11b and NN12b, respectively) through the Dacic Basin (Semenenko and Olejnik, 1995). We therefore propose that: (1) at Site 380, the Messinian beds presumably containing Mediterranean calcareous nannoplankton and dinoflagellate cysts were eroded during the desiccation phase, and (2) the post-desiccation (subzone NN12b) calcareous nannoplankton from the Crimea are coeval with the first marine dinoflagellate cysts and diatoms at Site 380 (i.e. 5.13 Ma, consistent with the temporal range of *Ceratolithus acutus*; Text-Figure 2). The fluvial erosion that dismantled the northern shelf of the Black Sea during the desiccation phase did not affect the Dobrogea horst (Gillet et al., 2003). The supposed obstacle of the Reni Strait (Text-

Figure 10A) was crossed again by marine Mediterranean waters at 5.13 Ma, which could explain the delayed migration of Zanclean marine Mediterranean calcareous nannoplankton, dinoflagellates, and diatoms into the Euxinian Basin (Schrader, 1978; Popescu, 2006).

In the Central Mediterranean, the first invasion by Paratethyan dinoflagellates occurred almost simultaneously as recorded at Eraclea Minoa, Cava Serredi, and Aghios Sostis on Zakynthos Island (Kontopoulos et al., 1997). This invasion relates only to the Mediterranean Basin itself as no record of this pre-desiccation ‘Lago Mare’ phase has ever been documented in the Adriatic–Po realm. The Paratethyan immigrants did not enter this realm before the desiccation phase probably because of important uplift in the area during the first stage of the Messinian Salinity Crisis (Scarselli et al., 2006). During the desiccation phase, the Adriatic–Po realm persisted as a suspended freshwater basin with a continuous clayey to turbiditic sedimentation in the Apennine foredeep (Clauzon et al., 1997, 2005; Scarselli et al., 2006). Simultaneously, Messinian marginal evaporites were reworked into the Apennine foredeep (Manzi et al., 2007). Owing to the well-dated succession of bioevents in the nannoplankton (Text-Figure 2), it is possible to refine the paleogeographic reconstruction by the precise timing of successive arrivals of Paratethyan dinoflagellates in the Mediterranean. The new Paratethyan immigrants arrived at 5.46 Ma in the Central Mediterranean as indicated by the Eraclea Minoa section, but they did not reach the Adriatic realm until about 115 kyr later (Text-Figure 7) when the Mediterranean sea-level was high enough to overflow the uplifting Otranto Sill (Text-Figure 10), a barrier created by the offshore extension of the Apulia shelf margin in conjunction with a major NE–SW transcurrent fault system (Clauzon et al., 1997).

To summarize, the role of straits and sills appears essential for deciphering paleogeographic changes in the crucial 8–5 Ma time-interval during which enormous changes in sea-level interplayed with intense tectonic movements. It has been possible to constrain the successive values of the Mediterranean sea-level during this time (Clauzon, 1996; 1999). Estimates are based on: (1) the global sea-level before the onset and after the end of the Messinian Salinity Crisis (i.e. when the Mediterranean was connected to the Atlantic Ocean) as given by Haq et al. (1987), and (2) meticulous field studies allowing the relative effects of sea-level change and regional tectonic movement throughout the Mediterranean (marginal and central basins) to be differentiated, including the interval during which it was isolated. These estimates are (see Text-Figure 2 for the precise chronology; asl–bsl = above–below the present global sea-level) (Clauzon, 1996; 1999; Clauzon et al., 1996):

- 1) 40 m asl at 6 Ma; ca. 110 m bsl between 5.96 and about 5.76 Ma, especially for marginal basins relatively isolated by sills (i.e. the marginal episode of the crisis);
- 2) 40 m asl between about 5.76 and 5.60 Ma, a sea-level rise mostly recorded in marginal basins (corresponding in particular to the Sicilian Upper Evaporites ending with the first ‘Lago Mare’ event at high sea-level; Text-Figure 1);
- 3) about 1500 m bsl between ca. 5.60 and 5.46 Ma (deep-basin episode of the crisis; see also: Savoye and Piper, 1991; Lofi et al., 2005; Sage et al., 2005);
- 4) 80 m asl at 5.332 Ma, after the post-Messinian Salinity Crisis reflooding (starting with the second ‘Lago Mare’ event at high sea-level).

Dinoflagellates are here shown to be highly effective organisms for establishing connection and/or isolation phases of the various basins adjacent to the Mediterranean. As the opposing migrations of Paratethyan and Mediterranean dinoflagellates must necessarily occur during phases of high sea-level, they are potentially useful for discriminating between the effects of local tectonic movements and regional sea-level changes. Among the Paratethyan dinoflagellate cysts, *Galeacysta etrusca* appears the most sensitive marker of the ‘Lago Mare’ events because its migration is narrowly linked to high sea-level phases. This is particularly true when comparing the vertical distribution of *Galeacysta etrusca* and dreissenids at Eraclea Minoa: *Galeacysta etrusca* is recorded in the relative high sea-level deposits represented by diatomitic turbidites preceding the highest gypsum bed and in the Arenazzolo Formation, while dreissenids occur within the Lago Mare Formation which corresponds to a relative lowering of sea-level (Text-Figure 4). As dreissenids may develop in invading coastal lagoon environments, they are more significant of local brackish conditions (possibly continuing after the invasion event) than *Galeacysta etrusca*, which precisely demarcates the exchange events at high sea-level between basins. *Galeacysta etrusca* appears also more effective in signaling such exchanges than ostracods of the *Cyprideis pannonica* group, as it shows a wider distribution in both space and time. These ostracods were used alone to define a dilution phase by river input recorded in the almost desiccated Mediterranean basins and ending the peak of the Messinian Salinity Crisis (McCulloch and De Deckker, 1989; Rouchy et al., 2001). This brief dilution event has been used wrongly to change the significance of the ‘Lago Mare’ events (Orszag-Sperber, 2006); it does not result from an exchange at high sea-level between the Mediterra-

nean and Paratethys but more probably represents a colonization of new freshwater habitats.

*Galeacysta etrusca* was also recorded in Late Pliocene deposits from ODP Site 898 in the Atlantic Ocean westward of the Iberian Peninsula coastline (McCarthy and Mudie, 1996). The authors invoke either a possible reworking or transport via the Mediterranean overflow water. As the published photograph (McCarthy and Mudie, 1996: pl. 2, fig. 12) is not entirely convincing, we are cautious of this record. However, it might be an extra-Mediterranean signal of a 'Lago Mare' event more recent than those discussed in this paper, a prospect not unrealistic if considering the almost continuous record of Mediterranean calcareous nannoplankton in the Dacic Basin up to Late Pliocene zone NN16 (MăruŃeanu and Papaianopol, 1995; 1998; Lourens et al., 2005). Indeed, the 'Lago Mare' events resulting from exchanges at high sea-level between the Mediterranean and Paratethys may have occurred at any time during the Late Neogene so long as a gateway was active between these basins. An older example of a Mediterranean–Paratethys connection was documented by Archambault-Guézou et al. (1979) based on a euxinic mollusc fauna found just below the Crevillente 6 mammal level in southeastern Spain, i.e. prior to 6.10 Ma (Garcés et al., 1998). This mollusc fauna shows affinities with the Maeotian mollusc fauna from the Eastern Paratethys (Archambault-Guézou et al., 1979).

## CONCLUSIONS

The high specificity of dinoflagellate cysts for reconstructing paleoenvironments is emphasized in this study, which reveals the extreme sensitivity of *Galeacysta etrusca*. Indeed, new biometric analyses and previously documented records of *Galeacysta etrusca* from the late Neogene of the Paratethys and Mediterranean allow us to reconstruct the history of this species within the framework of paleogeographic changes that occurred from 8 to 5 Ma. The associated chronology of calcareous nannoplankton bioevents, and the stratigraphic location of the studied deposits with respect to the isochronous Messinian Erosional Surface (formed at the peak of the Messinian Salinity Crisis), have together been particularly useful for depicting the chronological framework that underpins this study. This results in a reliable history of this species, especially regarding its significance as an immigrant from the Paratethys into the Mediterranean, its migration during high sea-level episodes (i.e. the 'Lago Mare' events), the timing of such episodes, and the locations and courses of the gateways.

*Galeacysta etrusca* originated in the Pannonian Basin in the Late Miocene. It invaded the Dacic Basin during the

interval 6–5.60 Ma, from where it migrated into the Mediterranean at least twice (major phases at ca. 5.60 and 5.46–5.278 Ma, i.e. just before and just after the peak of the Messinian Salinity Crisis, respectively), and later (at ca. 5.13 Ma) into the Black Sea.

Among the four statistically-defined stable biometric groups (Text-Figure 7), group 'a' appears to characterise brackish environments, accompanied by group 'c' when freshwater input increases, while group 'b' immediately replaces group 'a' when salinity increases. The large size of individuals in group 'd' developed in peculiar nutrient-rich conditions. This diversification into biometric groups developed irrespective of the realm (Paratethyan or Mediterranean) and period, with the possible exception of group 'd' which has presently been recorded only from the latest Messinian of the Adriatic.

From a paleogeographic perspective, the Portaferrian connection (6–5.60 Ma) between the Pannonian and Dacic basins is supported by this study, and its location specified: a Y-shaped corridor with two northern branches joining the Pannonian and Dacic basins together, and both to the Aegean Sea (Text-Figure 10A). The status of the Adriatic–Po realm as a suspended and isolated basin during the desiccation phase of the Mediterranean (as was probably the Dacic Basin in part) is supported by our data that document a delayed arrival (115 kyr) of *Galeacysta etrusca* compared to the Mediterranean Basin. The late arrival of the Mediterranean marine dinoflagellates accompanied by *Galeacysta etrusca* into the Black Sea at ca. 5.13 Ma confirms paleogeographic assumptions about its relationship with the nearby Dacic Basin (Text-Figure 10).

Finally, field observations (Text-Figure 4) and dinoflagellate cyst data indicate the reflooding of the Mediterranean Basin by Atlantic waters at ca. 5.46 Ma, i.e. significantly earlier than the GSSP of the Zanclean Stage at 5.332 Ma.

## ACKNOWLEDGMENTS

We are indebted to A. Bossio who provided his old photograph from Cava Serredi; to M.-A. Bassetti who provided her palynological residues from San Donato; to the late F. Marinescu and I. Papaianopol who guided J.-P.S and G.C. in 1998 at Cernat and Valea Vacii; and to the directors of the Cava Serredi Factory and Casabianda Prison who authorized several visits to the exposed deposits. The Ocean Drilling Program provided the samples from Site 380. The manuscript has been improved significantly by the comments of the reviewers, L.E. Edwards and W. Piller, and of F.M.G. McCarthy. This paper is a publication of the French Programs ECLIPSE II CNRS and ANR EGE0.

## References cited

- ARCHAMBAULT-GUÉZOU, J.  
1976 Présence de Dreissenidae euxiniques dans les dépôts à Congéries de la vallée du Rhône et sur le pourtour méditerranéen. Implications biogéographiques. *Bulletin de la Société Géologique de France*, ser. 7, 18(5): 1267–1276.
- ARCHAMBAULT-GUÉZOU, J., ILINA, L.B., KELLER, J.-P., and MONTENAT, C.  
1979 Affinités euxiniques des mollusques messiniens d'Elche (Alicante, Espagne) et implications paléogéographiques. *Annales Géologiques des Pays Helléniques*, hors série, 1: 27–37.
- BALTEŞ, N.  
1971 Pliocene Dinoflagellata and Acritarcha in Romania. In: Farinacci, A. (ed.), *Proceedings of the Second Planktonic Conference*, Rome 1970. Edizioni Tecnoscienza, Rome, Italy, p. 1–16.
- BASSETTI, M.A.  
1997 *Il Messiniano clastico post-evaporitico nelle Marche (Bacino Interno)*. Unpublished Ph.D. thesis, University of Bologna, Bologna, Italy, 163 p.
- BERTINI, A.  
2006 The northern Apennines palynological record as a contribute for the reconstruction of the Messinian palaeoenvironments. *Sedimentary Geology*, 188/189: 235–258.
- BERTINI, A., CORRADINI, D., and SUC, J.-P.  
1995 On *Galeacysta etrusca* and the connections between the Mediterranean and the Paratethys. *Romanian Journal of Stratigraphy*, 76(7): 141–142.
- BETHOUX, J.P., and GENTILI, B.  
1999 Functioning of the Mediterranean Sea: past and present changes related to freshwater input and climate changes. *Journal of Marine Systems*, 20: 33–47.
- BOSSIO, A., GIANNELLI, L., MAZZANTI, R., MAZZEI, R., and SALVATORINI, G.  
1981 Gli strati alti del Messiniano, il passaggio Miocene–Pliocene e la sezione plio-pleistocenica di Nugola nelle colline a NE dei Monti Livornesi. *Abstracts from the 9th Congress of the Società Paleontologica Italiana*, Pacini, Pisa, 1981: 55–90. [Excursion guide-book].
- BRAGA, J.C., MARTÍN, J.M., RIDING, R., AGUIRRE, J., SÁNCHEZ-ALMAZO, I.M., and DINARÈS-TURELL, J.  
2006 Testing models for the Messinian salinity crisis: The Messinian record in Almería, SE Spain. *Sedimentary Geology*, 188/189: 131–154.
- BROLSMA, M.J.  
1975 Lithostratigraphy and foraminiferal assemblages of the Miocene–Pliocene transitional strata of Capo Rossello and Eraclea Minoa (Sicily, Italy). *Proceedings of the Koninklijke Nederlandse Akademie Van Wetenschappen*, Series B, 78(5): 341–380.
- 1976 Discussion of the arguments concerning the palaeoenvironmental interpretation of the Arenazzolo in Capo Rossello and Eraclea Minoa (S. Sicily, Italy). *Memorie della Società Geologica Italiana*, 16: 153–157.
- BUTLER, R.W.H., LICKORISH, W.H., GRASSO, M., PEDLEY, H.M., and RAMBERTI, L.  
1995 Tectonics and sequence stratigraphy in Messinian basins, Sicily: Constraints on the initiation and termination of the Mediterranean salinity crisis. *Geological Society of America Bulletin*, 107: 425–439.
- CARNEVALE, G., LANDINI, W., and SARTI, G.  
2006 Mare versus Lago-Mare: marine fishes and the Mediterranean environment at the end of the Messinian Salinity Crisis. *Journal of the Geological Society of London*, 163: 75–80.
- CAVALLO, O., and REPETTO, G.  
1988 Un nuovo giacimento della facies a Congerie nell'Albese. *Rivista Piemontese di Storia Naturale*, 9: 43–62.
- CIESM (ANTÓN, J., ÇAÇATAY, M.N., DE LANGE, G., FLECKER, R., GAULLIER, V., GUNDE-CIMERMAN, N., HÜBSCHER, C., KRIJGSMAN, W., LAMBREGTS, P., LOFI, J., LUGLI, S., MANZI, V., McGENITY, T.J., ROVERI, M., SIERRO, F.J., and SUC J.-P.)  
2008 Executive summary. In: Briand, F. (ed.), *The Messinian Salinity Crisis from mega-deposits to microbiology – A consensus report. CIESM Workshop Monographs*, 33: 7–28.
- CITA, M.B., WRIGHT, R.C., RYAN, W.B.F., and LONGINELLI, A.  
1978 Messinian paleoenvironments. *Initial Reports of the Deep Sea Drilling Project*, 42(1): 1003–1035.
- CLAUZON, G.  
1996 Limites de séquences et évolution géodynamique. *Géomorphologie*, 1: 3–22.  
1999 L'impact des variations eustatiques du bassin de Méditerranée occidentale sur l'orogène alpin depuis 20 Ma. *Etudes de géographie physique*, 28: 1–8.
- CLAUZON, G., SUC, J.-P., GAUTIER, F., BERGER, A., and LOUTRE, M.-F.  
1996 Alternate interpretation of the Messinian salinity crisis: Controversy resolved? *Geology*, 24(4): 363–366.
- CLAUZON, G., RUBINO, J.-L., and CASERO, P.  
1997 Regional modalities of the Messinian Salinity Crisis in the framework of two phases model. *Abstracts from the R.C.M.N.S. Interim-Colloquium on Neogene basins of the Mediterranean region: controls*

- and correlation in space and time, Catania, November 1997: 44–46 (abstract).
- CLAUZON, G., SUC, J.-P., POPESCU, S.-M., MĂRUNȚEANU, M., RUBINO, J.-L., MARINESCU, F., and MELINTE, M.C.  
2005 Influence of the Mediterranean sea-level changes over the Dacic Basin (Eastern Paratethys) in the Late Neogene. The Mediterranean Lago Mare facies deciphered. *Basin Research*, 17: 437–462.
- CLAUZON, G., SUC, J.-P., DUMURDŽANOV, N., MELINTE-DOBRINESCU, M.C., and ZAGORCHEV, I.  
2008 The Pliocene Gilbert-type fan delta of Dračevo (Skopje area, Republic of Macedonia): Paleogeographic inference. *Geologica Macedonica*, 2: 21–28.
- CORNÉE, J.-J., CONESA, G., CLAUZON, G., FERRANDINI, M., FERRANDINI, J., GARCIA, F., MOISSETTE, P., MÜNCH, P., SAINT MARTIN, J.-P., SAINT MARTIN, S., RIBAUD, A., ROGER, S., SUC, J.-P., and VIOLANTI, D.  
2004 Late Messinian erosion and post-crisis reflooding in the Mediterranean: Constraints from marginal basins of NE Morocco, Sardinia and Sicily. Colloquium ‘The Messinian Salinity Crisis Revisited’, Corte, Poster, p. 28. <http://www.messinianonline.it/MSCCorte.php>
- CORRADINI, D., and BIFFI, U.  
1988 Etude des dinokystes à la limite Messinien–Pliocène dans la coupe Cava Serredi, Toscane, Italie. *Bulletin des Centres de Recherche Exploration-Production Elf-Aquitaine*, 12(1): 221–236.
- CORSELLI, C., and GRECCHI, G.  
1984 The passage from hypersaline to hyposaline conditions in the Mediterranean Messinian: Discussion of the possible mechanisms triggering the ‘Lago Mare’ facies. *Paléobiologie continentale*, 14(2): 225–239.
- COUR, P.  
1974 Nouvelles techniques de détection des flux et de retombées polliniques: étude de la sédimentation des pollens et des spores à la surface du sol. *Pollen et Spores*, 16(1): 103–141.
- CSATO, I., KENDALL, C.G.St C., and MOORE, P.D.  
2007 The Messinian problem in the Pannonian Basin, Eastern Hungary – Insights from stratigraphic simulations. *Sedimentary Geology*, 201: 111–140.
- DALE, B.  
1996 Dinoflagellate cyst ecology: modeling and geological applications. In: Jansonius, J., and McGregor, D.C. (eds.), *Palynology: Principles and Applications*. American Association of Stratigraphic Palynologists Foundation, Dallas, Texas, vol. 3, p. 1249–1276.
- DECIMA, A., and WEZEL, F.C.  
1971 Osservazioni sulle evaporiti messiniane della Sicilia centro-meridionale. *Rivista Mineraria Siciliana*, 22: 171–187.
- de VERNAL, A., GOYETTE, C., and RODRIGUES, C.G.  
1989 Contribution palynostratigraphique (dinokystes, pollen et spores) à la connaissance de la mer de Champlain: coupe de Saint Cezaire, Québec. *Canadian Journal of Earth Sciences*, 26: 2450–2464.
- DRIVALIARI, A., TICLEANU, N., MARINESCU, F., MĂRUNȚEANU, M., and SUC, J.-P.  
1999 A Pliocene climatic record at bicleni (Southwestern Romania). In: Wrenn, J.H., Suc, J.-P., and Leroy, S.A.G. (eds.), *The Pliocene: Time of Change*. American Association of Stratigraphic Palynologists Foundation, Dallas, Texas, p. 103–108.
- DUGGEN, S., HOERNLE, K., VAN DEN BOGAARD, P., RÜPKE, L., and MORGAN, J.P.  
2003 Deep roots of the Messinian salinity crisis. *Nature*, 422: 602–604.
- EL EUCH–EL KOUNDI, N., FERRY, S., SUC, J.-P., CLAUZON, G., MELINTE-DOBRINESCU, M.C., GORINI, C., SAFRA, A., and ZARGOUNI, F.  
2009 Messinian deposits and erosion in northern Tunisia: inferences on Strait of Sicily during the Messinian Salinity Crisis. *Terra Nova*, 21: 41–48.
- ELLEGAARD, M.  
2000 Variations in dinoflagellate cyst morphology under conditions of changing salinity during the last 2000 years. *Review of Palaeobotany and Palynology*, 109: 65–81.
- FAUQUETTE, S., SUC, J.-P., BERTINI, A., POPESCU, S.-M., WARNY, S., BACHIRI TAOUFIQ, N., PEREZ VILLA, M.-J., CHIKHI, H., FEDDI, N., SUBALLY, D., CLAUZON, G., and FERRIER, J.  
2006 How much did climate force the Messinian salinity crisis? Quantified climatic conditions from pollen records in the Mediterranean region. *Palaeogeography, Palaeoclimatology, Palaeoecology*, 238(1–4): 281–301.
- GARCÉS, M., KRIJGSMAN, W., and AGUSTÍ, J.  
1998 Chronology of the late Turolian deposits of the Fortuna basin (SE Spain): implications for the Messinian evolution of the eastern Betics. *Earth and Planetary Science Letters*, 163: 69–81.
- GAUTIER, F.  
1994 Calibration magnétostratigraphique du Messinien de la Méditerranée occidentale. Age, durée et déroulement de la crise de salinité. Unpublished Ph.D. thesis, Université Montpellier 2, Montpellier, France, 105 p.
- GILLET, H., LERICOLAIS, G., RÉHAULT, J.-P., and DINU, C.  
2003 La stratigraphie oligo–miocène et la surface d’érosion messinienne en mer Noire, stratigraphie sismique haute résolution. *Comptes Rendus Geoscience*, 335: 907–916.

- GILLET, H., LERICOLAIS, G., and RÉHAULT, J.-P.  
2007 Messinian events in the Black Sea: Evidence of a Messinian erosional surface. *Marine Geology*, 244: 142–165.
- GUIBOUT, P.  
1987 *Atlas hydrologique de la Méditerranée*. SDP IFREMER, Brest, 150 p.
- HAMMER, Ø., HARPER, D.A.T., and RYAN, P.D.  
2001 PAST: Paleontological statistics software package for education and data analysis. *Palaeontologia Electronica*, 4: 9 p.
- HAQ, B.U., HARDENBOL, J., and VAIL, P.R.  
1987 Chronology of fluctuating sea levels since the Triassic (250 million years ago to present). *Science*, 235: 1156–1167.
- HEAD, M.J.  
2007 Last Interglacial (Eemian) hydrographic conditions in the southwestern Baltic Sea based on dinoflagellate cysts from Ristinge Klint, Denmark. *Geological Magazine*, 144(6): 987–1013.
- HILGEN, F.J., and LANGEREIS, C.G.  
1993 A critical re-evaluation of the Miocene/Pliocene boundary as defined in the Mediterranean. *Earth and Planetary Science Letters*, 118: 167–179.
- HSÜ, K.J.  
1978 Stratigraphy of the lacustrine sedimentation in the Black Sea. *Initial Reports of the Deep Sea Drilling Project*, 42(2): 509–524.
- HSÜ, K.J., CITA, M.B., and RYAN, W.B.F.  
1973 The origin of the Mediterranean evaporites. *Initial Reports of the Deep Sea Drilling Project*, 13: 1203–1231.
- HSÜ, K.J., MONTADERT, L., BERNOULLI, D., CITA, M.B., ERICKSON, A., GARRISON, R.E., KIDD, R.B., MELIÈRES, F., MÜLLER, C., and WRIGHT, R.  
1978 History of the Mediterranean salinity crisis. *Initial Reports of the Deep Sea Drilling Project*, 42(1): 1053–1078.
- JOLIVET, L., AUGIER, R., ROBIN, C., SUC, J.-P., and ROUCHY, J.M.  
2006 Lithospheric-scale geodynamic context of the Messinian salinity crisis. *Sedimentary Geology*, 188/189, 9–33.
- KOJUMDGIEVA, E.  
1987 Evolution géodynamique du bassin Egéen pendant le Miocène Supérieur et ses relations à la Paratéthys Orientale. *Geologica Balcanica*, 17(1): 3–14.
- KOKINOS, J.P., and ANDERSON, D.M.  
1995 Morphological development of resting cysts in cultures of the marine dinoflagellate *Lingulodinium polyedrum* (= *L. machaerophorum*). *Palynology*, 19, 143–166.
- KONTOPOULOS, N., ZELILIDIS, A., PIPER, D.J.W., and MUDIE, P.J.  
1997 Messinian evaporites in Zakynthos, Greece. *Palaeogeography, Palaeoclimatology, Palaeoecology*, 129: 361–367.
- KOVÁČIČ, M., ZUPANIČ, J., BABIČ, L.J., VRDALJKO, D., MIKNIČ, M., BAKRAČ, K., HEČIMOVIĆ, I., AVANIĆ, R., and BRKIĆ, M.  
2004 Lacustrine basin to delta evolution in the Zagorje Basin, a Pannonian sub-basin (Late Miocene: Pontian, NW Croatia). *Facies*, 50: 19–33.
- KRÄUTNER, H.G., and KRSTIĆ, B.  
2003 *Geological map of the Carpatho-Balkanides between Mehadia, Oravița, Niš and Sofia*. Geoinstitut, Belgrade, map at a scale of 1/300,000.
- KRIJGSMAN, W., HILGEN, F.J., RAFFI, I., SIERRO, F.J., and WILSON, D.S.  
1999 Chronology, causes and progression of the Messinian salinity crisis. *Nature*, 400: 652–655.
- LEEVEER, K.  
2007 Foreland of the Romanian Carpathians. Controls on late orogenic sedimentary basin evolution and Paratethys paleogeography. Published Ph.D. thesis, NSG publication n° 20071204, Free University of Amsterdam, 182 p.
- LEGENDRE, P., and LEGENDRE, L.  
1998 *Numerical Ecology*. Elsevier, Amsterdam, 853 p.
- LEWIS, J., and HALLETT, R.  
1997 *Lingulodinium polyedrum* (*Gonyaulax polyedra*), a blooming dinoflagellate. *Oceanography and Marine Biology Annual Review*, 35: 97–161.
- LEWIS, J., ROCHON, A., and HARDING, I.  
1999 Preliminary observations of cyst–theca relationships in *Spiniferites ramosus* and *Spiniferites membranaceus* (Dinophyceae). *Grana*, 38: 113–124.
- LEWIS, J., ELLEGAARD, M., HALLETT, R., HARDING, I., and ROCHON, A.  
2003 Environmental control of cyst morphology in gonyaulacoid dinoflagellates. In: Matsuoka, K., Yoshida, M., and Iwataki, M. (eds.), Seventh International Conference on Modern and Fossil Dinoflagellates, Dino7, Nagasaki, Japan, September 21–25; Program, Abstracts, and Participants Volume, Additional Abstract.
- LOFI, J., GORINI, C., BERNÉ, S., CLAUZON, G., TADEU DOS REIS, A., RYAN, W.B.F., and STECKLER, M.S.  
2005 Erosional processes and paleo-environmental changes in the Western Gulf of Lions (SW France) during the Messinian Salinity Crisis. *Marine Geology*, 217: 1–30.
- LONDEIX, L., BENZAKOUR, M., SUC, J.-P., and TURON, J.-L.  
2007 Messinian paleoenvironments and hydrology in Sic-

- ily (Italy): The dinoflagellate cyst record. *Geobios*, 40(3): 233–250.
- LOURENS, L.J., HILGEN, F.J., LASKAR, J., SHACKLETON, N.J., and WILSON, D.  
2005 The Neogene Period. In: Gradstein, F., Ogg, J., and Smith, A. (eds.), *A geological time scale*. Cambridge University Press, p. 409–440. [Imprinted 2004]
- MAGYAR, I., GEARY, D.H., SÜTŐ-SZENTAI, M., LANTOS, M., and MÜLLER, P.  
1999a Integrated bio-, magneto- and chronostratigraphic correlations of the Late Miocene Lake Pannon deposits. *Acta Geologica Hungarica*, 42: 5–31.
- MAGYAR, I., GEARY, D.H., and MÜLLER, P.  
1999b Paleogeographic evolution of the Late Miocene Lake Pannon in Central Europe. *Palaeogeography, Palaeoclimatology, Palaeoecology*, 147: 151–167.
- MANZI, V., ROVERI, M., GENNARI, R., BERTINI, A., BIFFI, U., GIUNTA, S., IACCARINO, S.M., LANCI, L., LUGLI, S., NEGRI, A., RIVA, A., ROSSI, M.E., and TAVIANI, M.  
2007 The deep-water counterpart of the Messinian Lower Evaporites in the Apennine foredeep: the Fananello section (Northern Apennines, Italy). *Palaeogeography, Palaeoclimatology, Palaeoecology*, 251(3–4): 470–499.
- MARINESCU, F.  
1992 Les bioprovinces de la Paratéthys et leurs relations. *Paleontologia i Evolució*, 24–25: 445–453.
- MĂRUNȚEANU, M., and PAPAÏANOPOL, I.  
1995 The connection between the Dacic and Mediterranean Basins based on calcareous nannoplankton assemblages. *Romanian Journal of Stratigraphy*, 76(7): 169–170.  
1998 Mediterranean calcareous nannoplankton in the Dacic Basin. *Romanian Journal of Stratigraphy*, 78: 115–121.
- MCCARTHY, F.M.G., and MUDIE, P.J.  
1996 Palynology and dinoflagellate biostratigraphy of Upper Cenozoic sediments from Sites 898 and 900, Iberia abyssal plain. *Proceedings of the Ocean Drilling Program, Scientific Results*, 149: 241–265.
- MCCULLOCH, M.T., and De DECKKER, P.  
1989 Sr isotope constraints on the Mediterranean environment at the end of the Messinian salinity crisis. *Nature*, 342: 62–65.
- MEULENKAMP, J.E., and SISSINGH, W.  
2003 Tertiary palaeogeography and tectonostratigraphic evolution of the Northern and Southern Peri-Tethys platforms and the intermediate domains of the African–Eurasian convergent plate boundary zone. *Palaeogeography, Palaeoclimatology, Palaeoecology*, 196: 209–228.
- MÜLLER, P., GEARY, D.H., and MAGYAR, I.  
1999 The endemic molluscs of the late Miocene Lake Pannon: their origin, evolution, and family-level taxonomy. *Lethaia*, 32: 47–60.
- ORSZAG-SPERBER, F.  
2006 Changing perspectives in the concept of ‘Lago Mare’ in Mediterranean Late Miocene evolution. *Sedimentary Geology*, 188–189: 259–277.
- PILLER, W.E., HARZHAUSER, M., and MANDIC, O.  
2007 Miocene Central Paratethys stratigraphy – current status and future directions. *Stratigraphy*, 4(2–3): 151–168.
- POMEROL, C.  
1973 *Stratigraphie et paléogéographie. Ère Cénozoïque*. Doin, Paris: 269 p.
- POPESCU, S.-M.  
2001 Végétation, climat et cyclostratigraphie en Paratéthys centrale au Miocène supérieur et au Pliocène inférieur d’après la palynologie. Unpublished Ph.D. thesis, Université Lyon 1, Villeurbanne, France, 223 p.  
2006 Late Miocene and early Pliocene environments in the southwestern Black Sea region from high-resolution palynology of DSDP Site 380A (Leg 42B). *Palaeogeography, Palaeoclimatology, Palaeoecology*, 238(1–4): 64–77.
- POPESCU, S.-M., KRIJGSMAN, W., SUC, J.-P., CLAUZON, G., MĂRUNȚEANU, M., and NICA, T.  
2006 Pollen record and integrated high-resolution chronology of the early Pliocene Dacic Basin (southwestern Romania). *Palaeogeography, Palaeoclimatology, Palaeoecology*, 238(1–4): 78–90.
- POPESCU, S.-M., MELINTE, M.C., SUC, J.-P., CLAUZON, G., QUILLVERE, F., and SÜTŐ-SZENTAI, M.  
2007 Earliest Zanclean age for the Colombacci and uppermost Di Tetto formations of the ‘latest Messinian’ northern Apennines: New palaeoenvironmental data from the Maccarone section (Marche Province, Italy). *Geobios*, 40(3): 359–373.
- POPOV, S.V., SHCHERBA, I.G., ILYINA, L.B., NEVESSKAYA, L.A., PARAMONOVA, N.P., KHONDKARIAN, S.O., and MAGYAR, I.  
2006 Late Miocene to Pliocene palaeogeography of the Paratethys and its relation to the Mediterranean. *Palaeogeography, Palaeoclimatology, Palaeoecology*, 238(1–4): 91–106.
- RAFFI, I., BACKMAN, J., FORNACIARI, E., PÄLIKE, H., RIO, D., LOURENS, L., and HILGEN, F.  
2006 A review of calcareous nannofossil astro-biochronology encompassing the past 25 million years. *Quaternary Science Reviews*, 25: 3113–3137.

- REDNER, R.A., and WALKER, H.F.  
1984 Mixture Densities, Maximum Likelihood and the EM Algorithm. *SIAM Review*, 26(2): 195–239.
- RÖGL, F., and STEININGER, F.F.  
1983 Vom Zerfall der Tethys zu Mediterran und Paratethys. Die neogene Paläogeographie und Palinspastik des zirkum-mediterranen Raumes. *Annales des Naturhistorischen Museums in Wien*, 85(A): 135–163.
- ROUCHY, J.M., and CARUSO, A.  
2006 The Messinian salinity crisis in the Mediterranean basin: A reassessment of the data and an integrated scenario. *Sedimentary Geology*, 188–189: 35–67.
- ROUCHY, J.M., ORSZAG-SPERBER, F., BLANC-VALLERON, M.-M., PIERRE, C., RIVIÈRE, M., COMBOURIEU-NEBOUT, N., and PANAYIDES, I.  
2001 Paleoenvironmental changes at the Messinian–Pliocene boundary in the eastern Mediterranean: southern Cyprus basins. *Sedimentary Geology*, 145: 93–117.
- SACCHI, M., and HORVÁTH, F.  
2002 Towards a new time scale for the Upper Miocene continental series of the Pannonian basin (Central Paratethys). *EGU Stephan Mueller Special Publications Series*, 3: 79–94.
- SAGE, F., VON GRONEFELD, G., DEVERCHÈRE, J., GAULLIER, V., MAILLARD, A., and GORINI, C.  
2005 Seismic evidence for Messinian detrital deposits at the western Sardinia margin, northwestern Mediterranean. *Marine and Petroleum Geology*, 22: 757–773.
- SAINT MARTIN, S., SAINT MARTIN, J.-P., FERRANDINI, J., and FERRANDINI, M.  
2007 La microflore de diatomées au passage Mio–Pliocène en Corse. *Geobios*, 40(3): 375–390.
- SATTERTHWAITE, F.E.  
1946 An approximate distribution of estimates of variance components. *Biometrics Bulletin*, 2: 110–114.
- SAVOYE, B., and PIPER, D.J.W.  
1991 The Messinian event on the margin of the Mediterranean Sea in the Nice area, southern France. *Marine Geology*, 97: 279–304.
- SCARSELLI, S., SIMPSON, G.D.H., ALLEN, P.A., MINELLI, G., and GAUDENZI, L.  
2006 Association between Messinian drainage network formation and major tectonic activity in the Marche Apennines (Italy). *Terra Nova*, 19: 74–81.
- SCHRADER, H.-J.  
1978 Quaternary through Neogene history of the Black Sea, deduced from the paleoecology of diatoms, silicoflagellates, ebridians and chrysomonads. *Initial Reports of the Deep Sea Drilling Project*, 42(2): 789–901.
- SELLI, R.  
1973 An outline of the Italian Messinian. In: Drooger, C.W. (ed.), Messinian events in the Mediterranean. *Koninklijke Nederlandse Akademie Van Wetenschappen, Geodynamics Scientific Report 7*: 150–171.
- SEMENENKO, V.N., and OLEJNIK, E.S.  
1995 Stratigraphic correlation of the Eastern Paratethys Kimmerian and Dacian stages by molluscs, dinocyst and nannoplankton data. *Romanian Journal of Stratigraphy*, 76(7): 113–114.
- SIMPSON, G.G., ROE, A., and LEWONTIN, R.C.  
1960 *Quantitative Zoology*. Revised edition. Harcourt, Brace, and Company, New York, 440 p.
- SNEL, E., MĂRUNȚEANU, M., MACALEȚ, R., MEULENKAMP, J.E., and VAN VUGT, N.  
2006 Late Miocene to Early Pliocene chronostratigraphic framework for the Dacic Basin, Romania. *Palaeogeography, Palaeoclimatology, Palaeoecology*, 238(1–4): 107–124.
- SOKAL, R.R., and ROHLF, F.J.  
1995 *Biometry*. Third edition. Freeman and Co., New York, 887 p.
- STEVANOVIĆ, P.M.  
1951 Pontische Stufe im engeren Sinne – Obere Congerienschichten Serbiens und der angrenzenden Gebiete. *Serbische Akademie der Wissenschaften, Sonderausgabe, Mathematisch-Naturwissenschaftliche Klasse*, 2, 187: 1–351.
- 1974 Sur les échelles biostratigraphiques du Néogène marin et saumâtre de la Yougoslavie. *Mémoires du Bureau de Recherches Géologiques et Minières*, 78: 793–799.
- STOICA, M., LAZAR, I., VASILIEV, I., and KRIJGSMAN, W.  
2007 Mollusc assemblages of the Pontian and Dacian deposits from the Topolog-Argeș area (southern Carpathian foredeep – Romania). *Geobios*, 40(3): 391–405.
- SUC, J.-P., and BESSAIS, E.  
1990 Pérennité d'un climat thermo-xérique en Sicile, avant, pendant, après la crise de salinité messinienne. *Comptes Rendus de l'Académie des Sciences de Paris* (2), 310: 1701–1707.
- SÜTÖNÉ SZENTAI, M.  
1996 Micropaleontological type material of Natural Historical Collection at Komló. *Földtani Közlemény*, 126(2–3): 267–278.
- SÜTŐ-SZENTAI, M.  
1988 Microplankton zones of organic skeleton in the Pannonian *s.l.* stratum complex and in the upper part of the Sarmatian strata. *Acta Botanica Hungarica*, 34(3–4): 339–356.

- 1990 Mikroplanktonflora der pontischen (oberpannonischen) Bildungen Ungarns. *In*: Stevanović, P., Neveškaya, L., Marinescu, F., Sokač, A., and Jámbo, Á. (eds.), *Chronostratigraphie und Neostratotypen, Neogender Westlichen ('Zentrale') Paratethys*. Band VIII, Pontien. Jazu and Sanu, Zagreb–Belgrade, p. 842–869.
- 2000 Organic walled microplankton zonation of the Pannonian *s.l.* in the surroundings of Kaskantyú, Paks and Tengelic (Hungary). *Annual Report of the Geological Institute of Hungary, 1994–1995/III*, p. 153–175.
- SÜTŐ ZOLTÁNNÉ, M.
- 1994 Microplankton associations of organic skeleton in the surroundings of Villány Mts. *Földtani Közlöny*, 124(4): 451–478.
- TITTERINGTON, D., SMITH, A., and MAKOV, U.
- 1985 *Statistical analysis of finite mixture distributions*. John Wiley and Sons, Chichester, U.K., 254 p.
- VAN COUVERING, J.A., CASTRADORI, D., CITA, M.B., HILGEN, F.J., and RIO, D.
- 2000 The base of the Zanclean Stage and of the Pliocene Series. *Episodes*, 23(3): 179–187.
- VASILIEV, I., KRIJGSMAN, W., LANGEREIS, C.G., PANAIOTU, C.E., MAȚENCO, L., and BERTOTTI, G.
- 2004 Towards an astrochronological framework for the eastern Paratethys Mio–Pliocene sedimentary sequences of the Focșani basin (Romania). *Earth and Planetary Science Letters*, 227: 231–247.
- WALL, D., and DALE, B.
- 1974 Dinoflagellates in late Quaternary deep-water sediments from the Black Sea. *In*: Degens, E.T., and Ross, D.A. (eds.), *The Black Sea: Its Geology, Chemistry and Biology*. American Association of Petroleum Geologists, Memoir 20, p. 364–380.
- WALL, D., DALE, B., and HARADA, K.
- 1973 Descriptions of new fossil dinoflagellates from the late Quaternary of the Black Sea. *Micropaleontology*, 19: 18–31.
- WELCH, B.L.
- 1947 The generalization of 'student's' problem when several different population variances are involved. *Biometrika*, 34: 28–35.